Cardiomyocytes, cardiac endothelial cells and fibroblasts contribute to anthracycline-induced cardiac injury through RAS-homologous small GTPases RAC1 and CDC42

Pelin Kücük, Lena Abbey, Joachim Schmitt, Christian Henninger, Gerhard Fritz

Pharmacological Research 203 (2024) 107165

Contents lists available at ScienceDirect

Pharmacological Research

journal homepage: www.elsevier.com/locate/yphrs

Cardiomyocytes, cardiac endothelial cells and fibroblasts contribute to anthracycline-induced cardiac injury through RAS-homologous small GTPases RAC1 and CDC42

Pelin Kücük [a,*], Lena Abbey [a], Joachim Schmitt [b], Christian Henninger [a], Gerhard Fritz [a,*]

[a] Institute of Toxicology, Medical Faculty and University Hospital Düsseldorf, Heinrich Heine University Düsseldorf, Moorenstrasse 5, Düsseldorf 40225, Germany
[b] Institute of Pharmacology, Medical Faculty and University Hospital Düsseldorf, Heinrich Heine University Düsseldorf, Moorenstrasse 5, Düsseldorf 40225, Germany

ARTICLE INFO

Keywords:
Anthracyclines
Cardiotoxicity
RHO GTPases
DNA damage
DNA damage response

ABSTRACT

The clinical use of the DNA damaging anticancer drug doxorubicin (DOX) is limited by irreversible cardiotoxicity, which depends on the cumulative dose. The RAS-homologous (RHO) small GTPase RAC1 contributes to DOX-induced DNA damage formation and cardiotoxicity. However, the pathophysiological relevance of other RHO GTPases than RAC1 and different cardiac cell types (i.e., cardiomyocytes, non-cardiomyocytes) for DOX-triggered cardiac damage is unclear. Employing diverse in vitro and in vivo models, we comparatively investigated the level of DOX-induced DNA damage in cardiomyocytes versus non-cardiomyocytes (endothelial cells and fibroblasts), in the presence or absence of selected RHO GTPase inhibitors. Non-cardiomyocytes exhibited the highest number of DOX-induced DNA double-strand breaks (DSB), which were efficiently repaired in vitro. By contrast, rather low levels of DSB were formed in cardiomyocytes, which however remained largely unrepaired. Moreover, DOX-induced apoptosis was detected only in non-cardiomyocytes but not in cardiomyocytes. Pharmacological inhibitors of RAC1 and CDC42 most efficiently attenuated DOX-induced DNA damage in all cell types examined in vitro. Consistently, immunohistochemical analyses revealed that the RAC1 inhibitor NSC23766 and the pan-RHO GTPase inhibitor lovastatin reduced the level of DOX-induced residual DNA damage in both cardiomyocytes and non-cardiomyocytes in vivo. Overall, we conclude that endothelial cells, fibroblasts and cardiomyocytes contribute to the pathophysiology of DOX-induced cardiotoxicity, with RAC1- and CDC42-regulated signaling pathways being especially relevant for DOX-stimulated DSB formation and DNA damage response (DDR) activation. Hence, we suggest dual targeting of RAC1/CDC42-dependent mechanisms in multiple cardiac cell types to mitigate DNA damage-dependent cardiac injury evoked by DOX-based anticancer therapy.

1. Introduction

The anthracycline family of anticancer drugs is extensively used in the treatment of breast cancer, sarcoma, lymphoma and various childhood malignancies [1]. Anthracyclines act as topoisomerase II (TOP2) poisons, which inhibit the re-ligation activity of the enzyme, thus leading to the formation of DNA double-strand breaks (DSB) [2]. DSB are highly cytotoxic DNA lesions and potent triggers of the DNA damage response (DDR), which plays a key role in the regulation of cell survival and death [3]. In addition, generation of reactive oxygen species (ROS), DNA intercalation, inhibition of DNA helicases and chromatin damage also contribute to the cytotoxicity of anthracyclines [4,5]. Irreversible cardiotoxicity that can lead to cardiomyopathy and congestive heart failure (CHF) is the clinically most relevant dose-limiting adverse effect

Abbreviations: α-SMA, smooth muscle actin; BW, body weight; CDC42, cell division cycle 42; CHF, congestive heart failure; CHK1/2, checkpoint kinase 1/2; cTnI/T, cardiac troponin I/T; DAPI, 4`,6-diamidino-2-phenylindole; DDR, DNA damage response; DOX, doxorubicin; DSB, DNA double-strand breaks; ETO, etoposide; GAP, GTPase activating proteins; GAPDH, glyceraldehyde-3-phosphate dehydrogenase; GEF, guanine nucleotide exchange factors; γH2AX, phosphorylated histone H2AX (serine 139); HMG-CoA, 3-hydroxy-3-methylglutaryl-coenzyme A; IC_{50}, inhibitory concentration 50%; IR, ionizing radiation; KAP1, KRAB-associated protein-1; MAPK, mitogen-activated protein kinase; MEF, mouse embryonic fibroblasts; NF-κB, nuclear factor kappa B; RAC1, RAS-related C3 botulinum toxin substrate 1; RHO, RAS-homologous; ROS, reactive oxygen species; TOP2, topoisomerase II; TUNEL, terminal deoxynucleotidyl transferase dUTP nick end labeling; WGA, wheat germ agglutinin.

* Correspondence to: Institute of Toxicology, Heinrich Heine University Düsseldorf, Moorenstrasse 5, Düsseldorf 40225, Germany
E-mail addresses: kuecuekt@uni-duesseldorf.de (P. Kücük), fritz@uni-duesseldorf.de (G. Fritz).

https://doi.org/10.1016/j.phrs.2024.107165
Received 23 October 2023; Received in revised form 1 March 2024; Accepted 29 March 2024
Available online 30 March 2024

of anthracyclines, which depends on their cumulative dose and may occur early or late after treatment [1]. Due to its diverse toxic mechanisms of action, the pathophysiology of DOX-induced cardiotoxicity is rather complex. As concluded from the low antioxidative capacity of cardiomyocytes, the generation of ROS by mitochondria-related iron--dependent and -independent mechanisms are likely to play a significant role in the pathophysiology of DOX-induced cardiac damage, involving the activation of NF-kB-related pro-inflammatory and pro-fibrotic stress responses, inhibition of pro-survival AKT signaling and stimulation of p53-regulated mechanisms of senescence and cell death [6–10]. Hence, studies aiming to develop cardioprotective strategies mainly focused on the prevention of anthracycline-mediated ROS production and oxidative stress responses [9–11]. However, it appears that antioxidants do not have a substantial protective effect against cardiac damage caused by anthracyclines [4,12,13]. By contrast, efficient prophylaxis of anthracycline-induced cardiotoxicity can be achieved by use of dexrazoxane [14]. As concluded from experiments using chemical derivatives of dexrazoxane, it is hypothesized that the prevention of anthracycline-induced cardiotoxicity by dexrazoxane is independent of its iron chelating activity, but rather is mediated by inhibition of TOP2, in particular the TOP2B isoform [15,16]. In line with this hypothesis, genetic knockout of TOP2B prevented anthracycline-induced cardiotoxicity in vivo [15]. Due to increased incidence of secondary leukemias [17] and possible impairment of the anticancer efficacy of anthracyclines [18], the clinical use of dexrazoxane was restricted by the FDA in 2011. Hence, there is a clear clinical need for novel and well-tolerated drugs that lower the risk of cardiac dysfunction in the context of anthracycline-based anticancer therapy.

HMG-CoA (3-hydroxy-3-methylglutaryl-coenzyme A) reductase inhibitors (statins) have been reported to protect against the cardiotoxic effects of anthracycline derivatives (e.g., doxorubicin (DOX)) in in vitro and in vivo model systems [19,20] and, moreover, have also been reported to be effective in clinical trials [21]. Statins inhibit cholesterol biosynthesis through depletion of isoprene precursors, which are required for posttranslational modifications of small GTP-binding proteins of the RAS-homologous (RHO) family [22]. Particularly RAC1 (RAS-related C3 botulinum toxin substrate 1) was shown to be a relevant target for the pleiotropic (i.e., cholesterol-independent) cardioprotective effects of statins [20,22,23]. This might be related to the involvement of RAC1 in the regulation of the activity of NADPH oxidase, protein kinases (e.g., MAPK, AKT), transcription factors (e.g., NF-κB, AP1, STATs) as well as cell adhesion and cell death-related factors [24–27]. In addition, DOX-induced activation of NF-κB-regulated expression of pro-inflammatory and pro-fibrotic cytokines was attenuated by lovastatin [28–30]. Similar to statins, RAC1-specific small--molecule inhibitors, such as NSC23766 [31] and EHT1864 [32] mitigated DOX-induced geno- and cytotoxicity in vitro, as well as cardiac damage in vivo [20,23,33,34]. It has been hypothesized that this is due to an interference of RAC1-signaling with the DOX-induced formation of the TOP2-DNA cleavable complex [33,35]. Overall, the available preclinical data suggest that RAC1-regulated mechanisms are promising therapeutic targets for the prevention of cardiac damage evoked by anthracyclines. However, the contribution of other RHO GTPases than RAC1 to DOX-triggered cardiotoxicity is still unknown. Moreover, it is still largely unclear which cardiac cell types are of particular relevance for the pathophysiology of anthracycline-induced damage and the geno- and cytoprotective effects mediated by statins or RAC1 inhibitors. To our best knowledge, a detailed comparative analysis of the anthracycline response of cardiomyocytes versus non-cardiomyocytes is not yet available. Noteworthy in this context, a cardiomyocyte specific genetic deletion of Rac1 partially attenuated subacute cardiac damage observed at a later time point after repeated anthracycline treatment but not acute injury as detected at early time point after single exposure [36]. Hence, it is feasible that the involvement of certain cardiac cell types and RAC1-regulated pathophysiological mechanisms in anthracycline-induced cardiotoxicity depend on the time period and the doses applied [37]. Accordingly, it is tempting to speculate that the extent of DOX-induced DNA damage formation at early time point after anthracycline exposure, resulting in a time-dependent development of cardiac dysfunction, involves multiple cardiac cell types and different RHO-regulated signaling pathways.

To address these issues in more detail, we investigated (i) the susceptibility of different cardiac cell types to anthracycline-induced DNA damage as well as (ii) the relevance of different RHO GTPase-regulated signaling pathways in these cell types. To this end, we comparatively analyzed the formation of DNA damage (i.e., DSB) and its repair in different established and primary murine cardiac cell types (i.e., cardiomyocytes, endothelial cells, fibroblasts) following DOX treatment. Furthermore, we investigated the modulatory effects of selective pharmacological inhibitors of RHO GTPases on DOX-induced DNA damage formation and related cellular stress responses as reflected by the activation of selected DDR factors. The in vitro studies were complemented by in vivo analyses, where the influence of pharmacological inhibition of RHO GTPase signaling on DNA damage formation evoked by DOX treatment was comparatively investigated in cardiomyocytes versus non-cardiomyocytes.

2. Methods

2.1. Cell lines

Immortalized HL-1 cardiomyocytes from W.C. Claycomb (New Orleans, LA, USA) [38] were grown on gelatine (2 mg/ml)/fibronectin (1 mg/ml) (Sigma Aldrich, Darmstadt, Germany) coated dishes and maintained in Claycomb medium, supplemented with 10% FBS and 100 μM norepinephrine (Sigma Aldrich, Darmstadt, Germany). Immortalized H5V cardiac endothelial cells from A. Vecchi (Rozzano, Italy) [39] were maintained in DMEM supplemented with 10% FBS. Mouse embryonic fibroblasts (MEF (C57BL/6) [MEF-BL/6–1]) were purchased from ATCC® (SCRC1008™) and maintained in DMEM supplemented with 15% FBS. All cell cultures were maintained at 37 °C with 5% CO_2 containing humidified atmosphere. Experiments were performed with the cell lines at maximum passage number 40 for HL-1, 15 for H5V and 20 for MEF cells.

2.2. Isolation and culture of primary cardiac cell types

Primary cardiac cells were isolated from 8 to 12 weeks old C57BL/6 mice using Langendorff perfusion system as previously described [40]. Briefly, isolated hearts were cannulated to a blunted 23 G needle via the aorta and perfused with perfusion buffer (113 mM NaCl, 4.7 mM KCl, 0.6 mM KH_2PO_4, 0.6 mM Na_2HPO_4, 1.2 mM $MgSO_4$, 12 mM $NaHCO_3$, 10 mM $KHCO_3$, 10 mM HEPES, 30 mM taurine, 10 mM glucose, 0.01 mM blebbistatin (MedChemExpress, Monmouth Junction, NJ, USA), pH 7.2) at 37 °C with a flow rate of 3 ml/min for 5 min and subsequently perfused with enzyme buffer containing 300 U/ml collagenase II (Worthington Biochemical Corporation, Lakewood, NJ, USA) and 0.013 mg/ml protease XIV (Sigma Aldrich, Darmstadt, Germany) for 10 min. After enzymatic digestion, hearts were minced into small pieces and pipetted several times using a plastic Pasteur pipette to facilitate cell dissociation. Cell suspension was transferred to 50 ml tubes through a 300 μm cell strainer (pluriSelect Life Science UG, Leipzig, Germany). Ca^{2+} was reintroduced gradually to reach a concentration of 1 mM. Cells were centrifuged at 30 xg for 3 min. The cardiomyocyte containing pellet was resuspended and maintained in M199 medium (Thermo Fisher Scientific, Waltham, MA, USA) containing 5 mM creatine, 2 mM carnitine, 5 mM taurine, 0.01 mM blebbistatin, 1% insulin-transferrin-selenium (Thermo Fisher Scientific, Waltham, MA, USA) and 1% lipid mixture (Sigma Aldrich, Darmstadt, Germany) and seeded on 25 μg/ml laminin (Sigma Aldrich, Darmstadt, Germany) coated petri dishes. Supernatant consisting of non-cardiomyocytes was transferred to new falcon tubes and centrifuged at 300 xg for 5 min. For

the enrichment of endothelial cells, non-cardiomyocytes were resuspended in endothelial cell growth medium (PromoCell, Heidelberg, Germany) and seeded on laminin-coated culture dishes. For fibroblast cultures, cells were resuspended in DMEM F12 (Thermo Fisher Scientific, Waltham, MA, USA) supplemented with 10% FBS. Cell types were characterized by immunocytochemical analyses using cell type-specific antibodies, i.e., anti-cardiac troponin T (cTnT) (#564766, BD Biosciences, Franklin Lakes, NJ, USA) or anti-cardiac troponin I (cTnI) (#ZRB1355, Sigma Aldrich, Darmstadt, Germany) (1:2000) for cardiomyocytes, anti-CD31 for endothelial cells and anti-alpha smooth muscle actin (α-SMA) (#ab124432, Abcam, Cambridge, UK) or anti-vimentin (#5741, Cell Signaling, Beverly, MA, USA) (1:200) for fibroblasts.

2.3. Animal experiments

C57BL/6 mice were maintained in the central animal facility of the Heinrich Heine University Düsseldorf (ZETT). Animal experiments were conducted in accordance with the European Guidelines for the Care and Use of Laboratory Animals (2010/63/EU) and were approved by the national authority (North Rhine-Westphalia State Agency for Nature, Environment and Consumer Protection (approval reference number: 84–02–04.2011.A183)). 8–10 weeks old male and female mice (20–25 g BW) were used at a group size of 3–6 animals per experimental group. Mice were treated with repeated low doses (i.e., subacute) of DOX, in the presence or absence of RHO GTPase inhibitors. Treatment scheme was performed as follows: NSC23766 (5 mg/kg BW, i.p.) (Tocris, Wiesbaden-Nordenstadt, Germany) or lovastatin (10 mg/kg BW, p.o.) (Calbiochem, Darmstadt, Germany) were administered at three consecutive days before repeated DOX treatments (6 ×3 mg/kg BW, i.p.), and three times a week during DOX treatments. DOX or saline were injected twice a week for a total of three weeks. Six days after the last DOX injection, necropsy was performed under ketamine (100 mg/kg BW, i.p.) (Zoetis, NJ, USA) / xylazine (10 mg/kg BW, i.p.) (Bayer, Leverkusen, Germany) anesthesia. Hearts were isolated and fixed in formalin and embedded in paraffin for immunohistochemical analyses [34].

2.4. Analysis of cell cycle distribution

Analysis of cell cycle distribution was performed 24 h after DOX pulse-treatment (1 μM, 2 h). After trypsinization, cells were washed with PBS and fixed in 70% ethanol. Nuclear DNA was stained with propidium iodide (PI) (5 μg/ml) (Sigma Aldrich, Darmstadt, Germany), containing RNase A (100 mg/ml) (Serva Electrophoresis, Heidelberg, Germany) in PBS. Cell cycle distribution was assessed by flow cytometry using BD Accuri™ C6 (Becton Dickinson, NJ, USA) flow cytometer. The percentage of cells present in the different phases of the cell cycle were calculated. Moreover, SubG1 fraction was analyzed as marker of apoptotic fraction.

2.5. Immunofluorescence microscopy

For immunocytochemical analyses, cells were fixed on glass coverslips using 4% paraformaldehyde in PBS and were permeabilized with 0.5% Triton X-100 in PBS. After blocking with 5% bovine serum albumin (BSA) in PBS, cells were incubated with primary antibodies (1.5 h; RT) and subsequently with Alexa Fluor™-conjugated secondary antibodies (#A11008, #A11001 or #A21428 Invitrogen, Waltham, MA, USA) (1:600) for 1 h at RT. For immunohistochemical analyses, formalin-fixed paraffin-embedded heart tissues were cut into 3 μm sections using a Hyrax M25 microtome (Carl Zeiss, Jena, Germany), de-paraffinized and rehydrated in a graded series of ethanol. Sections were subjected to antigen retrieval with citrate buffer and blocked for 2 h with protein block (Dako, Hamburg, Germany) prior to incubation with primary antibody (overnight; 4 °C). After incubation with secondary antibody (2 h; RT), Alexa Fluor™-conjugated WGA (wheat germ agglutinin; 10 μg/ml) (Sigma Aldrich, Darmstadt, Germany) was used to stain cell membranes in order to morphologically distinguish between cardiomyocytes and non-cardiomyocytes. Cells or tissue sections were mounted using the blue fluorescent DNA stain DAPI (4`,6-diamidino-2-phenylindole) containing PromoFluor antifade mounting medium (PromoKine, Heidelberg, Germany). Microscopical analysis was performed using an Olympus BX 43 microscope (Olympus, Hamburg, Germany).

2.6. Analysis of DOX-induced DNA damage formation

Induction and repair of DNA double-strand breaks (DSB) was monitored by microscopical analysis of nuclear foci formed by Ser139 phosphorylated histone H2AX (γH2AX foci) as surrogate marker of DSB [41]. Immortalized cells were pulse-treated with DOX (0.2–1 μM) or etoposide (ETO) (2–10 μM) (Sigma Aldrich, Darmstadt, Germany) for 1 h. Subsequently the cell layer was washed with PBS and cells were further incubated in drug-free medium. In case of ionizing radiation (IR), cells were irradiated with 2–5 Gy IR in Gammacell® 1000 Elite (Cs^{137} source) and analyses were performed 0.5 h after exposure. DSB formation and repair were assessed in primary cardiac cells after 2 h DOX pulse-treatment (1 μM DOX), followed by a post-incubation period of up to 24 h in drug-free medium. For the inhibition of RHO GTPases, cells were pre-treated with following inhibitors: EHT1864 (30 μM), NSC23766 (100 μM), rhosin (100 μM) (Tocris, Wiesbaden-Nordenstadt, Germany), EHop-016 (10 μM), ML141 (100 μM), Y-27632 (10 μM) (Sigma Aldrich, Darmstadt, Germany), Aza1 (10 μM) (MedChemExpress, Monmouth Junction, NJ, USA) for 3 h; lovastatin (20 μM) overnight, prior to DOX treatment for 2 h. Specificity and mode of action of RHO GTPase inhibitors are shown in **Supplementary Table 1**. Nuclear γH2AX and/or 53BP1 foci were detected by immunofluorescence microscopy using anti-phospho-H2AX (Ser139) antibody (#05–636) (Merck Millipore, Darmstadt, Germany) (1:1000) or anti-phospho-H2AX (Ser139) antibody (#9718) and anti-53BP1 antibody (#4937) (Cell Signaling, Beverly, MA, USA) (1:500).

2.7. Knockdown of Rac1 and Cdc42 by siRNA transfection

To confirm data obtained by use of pharmacological inhibitors of the RHO GTPases RAC1 and CDC42, their mRNA expression was downregulated by siRNA-based genetic approach as previously described [42]. To this end, cells were transfected with siRNA directed against Rac1 and Cdc42 (QIAGEN, Hilden, Germany), using Lipofectamine RNAiMAX (Thermo Fisher Scientific, Waltham, MA, USA) as transfection reagent. siRNA sequences are given in **Supplementary Table 2**. Control samples were transfected with scrambled siRNA. 72 h after siRNA transfection, cells were treated with 1 μM DOX for 2 h. Subsequently, cells were fixed for immunofluorescent detection of γH2AX foci and proteins were extracted to analyze the protein expression of RAC1, CDC42 and selected factors of the DDR by western blot.

2.8. Analysis of cell viability and apoptosis

Established cell lines and primary cardiac cells were treated with DOX (0.1–5 μM) for 24–72 h. In case of pharmacological RAC1 inhibition, cells were pulse-treated with EHT1864 (30 μM) for 3 h. After washing with PBS, DOX was administered, and cells were incubated in the absence of EHT1864 before cell viability was analyzed using the AlamarBlue™ assay. To this end, cells were incubated with 44 μM resazurin sodium salt in DMEM w/o phenol red (Sigma Aldrich, Darmstadt, Germany) for 2–4 h and the reduction of non-fluorescent resazurin to fluorescent resorufin was measured at 535 nm excitation/590 nm emission using Infinite F200 microplate reader (TECAN, Männedorf, Switzerland). Resorufin fluorescence intensity of untreated controls was set to 100%. Apoptotic cell fraction was quantified by TUNEL (terminal deoxynucleotidyl transferase dUTP nick end labeling) assay (Roche

Diagnostics, Mannheim, Germany) after 1 μM DOX treatment for 48 h, with or without EHT1864 pulse-treatment (30 μM; 3 h). Briefly, fluorescein-conjugated dUTP nucleotides were transferred to the free 3′-OH groups in fragmented DNA in apoptotic cells by terminal deoxynucleotidyl transferase enzyme. TUNEL positive cells were visualized by immunofluorescence microscopy.

2.9. Determination of cellular ROS levels by 2`,7`-dichlorofluorescin diacetate (DCFDA) assay

Established cell lines were treated with 20 μM DCFDA (Abcam, Cambridge, UK) for 45 min prior to EHT1864 (30 μM) treatment for 3 h and subsequent DOX (1 μM and 10 μM) co-treatment for 2 h. The level of fluorescent 2`, 7`-dichlorofluorescein (DCF), which is indicative of the formation of ROS, was measured at 485 nm excitation/535 nm emission using Infinite F200 microplate reader. For positive control, cells were treated with tert-butylhydroperoxide (TBHP) (250 μM). DOX-induced increase in fluorescence was related to that of untreated control which was set to 100%.

2.10. Western blot analyses

After pre-treatment with RHO GTPase inhibitors (or siRNA transfection) and DOX co-treatment for 2 h, as described above, proteins were extracted with RIPA lysis buffer (50 mM Tris–HCl, 150 mM NaCl, 2 mM EDTA, 1% NP-40, 0.1% sodium dodecyl sulphate (SDS), 1% sodium deoxycholate, 1 mM sodium orthovanadate, 50 mM sodium fluoride, 1 mM phenylmethanesulfonylfluoride and 1% protease inhibitor cocktail (Cell Signaling, Beverly, MA, USA)). Samples were sonicated and protein concentration was determined by the DC™ Protein Assay (Bio-Rad Laboratories, Hercules, CA, USA). Protein samples were diluted in loading buffer (Roth, Karlsruhe, Germany) and denatured at 95 °C for 5 min. Proteins were separated by SDS-PAGE and transferred onto nitrocellulose membranes (GE Healthcare, Freiburg, Germany). After blocking with 5% BSA in 0.1% Tween 20 (Sigma Aldrich, Darmstadt, Germany) in TBS, membranes were incubated with primary antibodies: anti-phospho-p53 (S15) (#9284); anti-phospho-CHK1 (S345) (#2341); anti-phospho-CHK2 (T68) (#2661); anti-GAPDH (#2118) (Cell Signaling, Beverly, MA, USA) (1:1000); anti-phospho-H2AX (Ser139) (#05–636); anti-Rac1 (#05–389) (Merck Millipore, Darmstadt, Germany) (1:1000); anti-Cdc42 (#sc-8401) (Santa Cruz Biotechnology, Dallas, TX, USA) (1:200); anti-phospho-KAP1 (S824) (#A300–767A) (Bethyl Laboratories, Montgomery, TX, USA) (1:1000) overnight at 4 °C and subsequently with HRP-conjugated secondary antibodies (#610–1302 or #611–1302) (Rockland Immunochemicals, Limerick, PA, USA) (1:2000). Protein expression of GAPDH was used as loading control. Chemiluminescence imaging was performed using the Chem-iDoc™ Imaging System (Bio-Rad Laboratories, Hercules, CA, USA).

2.11. Statistical analyses

For statistical analyses one-way ANOVA with Bonferroni's post-hoc test was used (GraphPad Prism v6 (San Diego, CA, USA)). p-values ≤ 0.05 were considered statistically significant and marked as indicated in the legends to the figures. All data are presented as mean + SD calculated from at least three independent experiments as specified in the legends to the figures.

3. Results

3.1. DOX-induced cytotoxicity, DSB formation and repair in established murine cardiac cell models in vitro

Established murine cell lines (i.e., HL-1 cardiomyocytes, H5V cardiac endothelial cells, and mouse embryonic fibroblasts (MEF)) were employed for initial analyses of drug-induced cyto- and genotoxicity. Immunocytochemical analyses showed that HL-1 cardiomyocytes, H5V endothelial cells and MEF expressed cell type-specific protein markers (i.e., cardiomyocytes, cTnT; endothelial cells, CD31; mouse fibroblasts, α-SMA) as anticipated (Fig. 1**a**). Evaluating cell cycle distribution following DOX treatment, we observed that HL-1 cardiomyocytes exhibited the most pronounced G2/M arrest (~60% of cells in G2/M), while H5V endothelial cells showed the strongest increase in the percentage of apoptotic cells present in the subG1 fraction (Fig. 1**b**). To monitor DOX-induced cytotoxicity, cell viability was evaluated by use of the AlamarBlue™ assay. We observed that, after short-term DOX exposure (i.e., 24 h) as well as after extended exposure time (i.e., 72 h) with low DOX concentration (i.e., 0.1 μM and 0.2 μM), HL-1 cardiomyocytes were more resistant to DOX (IC_{50}: ~0.3 μM) than H5V endothelial cells and MEF (IC_{50}: <0.1 μM each) (Fig. 1**c left and right panel**). At later time point of analysis (i.e., 72 h), high concentration of DOX (i.e., 0.5 μM and 1 μM) caused stronger cytotoxicity in HL-1 and MEF as compared to H5V cells (Fig. 1**c right panel**).

DOX-induced formation and repair of DNA damage were monitored after DOX pulse-treatment (1 μM, 1 h) by analyzing the number of nuclear γH2AX foci as surrogate marker of DSB. The DSB inducing TOP2 inhibitor etoposide (ETO) (10 μM) and ionizing radiation (IR) (5 Gy), which is another prototypical DSB inducing agent, were included in the analyses as additional controls (Fig. 1**d-f**). As analyzed immediately after the DOX pulse-treatment (i.e., 0 h), HL-1 cardiomyocytes exhibited the lowest number of DOX-induced nuclear γH2AX foci (~5 foci per nucleus) as compared to H5V endothelial cells and MEF (~ 15 γH2AX foci and ~10 γH2AX foci per nucleus, respectively) (Fig. 1**d-f**). Similar results were obtained following ETO or IR exposure (Fig. 1**d-f**). The time-dependent reduction of γH2AX foci over a post-treatment period of 24 h, which reflects DSB repair capacity, revealed a largely impaired repair of DOX-induced DSB in HL-1 cardiomyocytes, while both ETO- and IR-induced DSB were efficiently repaired (Fig. 1**d**). By contrast, both H5V endothelial cells and MEF repaired approximately 50–80% of DOX-induced DSB (Figs. 1**e and** 1**f**). Moreover, both types of non-cardiomyocyte cell types efficiently repaired DSB formed after ETO- and IR-exposure (Figs. 1**e and** 1**f**). Basically, identical results were obtained when the three different cell types were exposed to lower concentrations of DOX, ETO, or IR **(Supplementary Fig. 1)**. Overall, the data indicate substantial cell type-specific differences in the formation and repair of DOX-induced DSB.

3.2. Impact of the pharmacological inhibition of RHO GTPase-regulated signaling pathways on anthracycline-induced DNA damage response (DDR) in established cell lines in vitro

Next, we investigated the outcome of the pharmacological inhibition of various types of RHO GTPases with regard to DOX-induced DSB formation. To this end, pharmacological inhibitors known to block RAC1-, CDC42- or RHOA-regulated signaling pathways by different mode of action **(Supplementary Table 1)** were employed. After pre-treatment with the corresponding inhibitors, cells were exposed to DOX (1 μM, 2 h) before analyses were performed. Once more, a relatively low number of nuclear γH2AX foci were formed in HL-1 cardiomyocytes as compared to H5V and MEF **(Supplementary Fig. 2a**), supporting the hypothesis that DOX-induced formation of DSB is particularly low in cardiomyocytes. Among the different RHO GTPase inhibitors tested, the pan RHO inhibitor lovastatin (20 μM) and the CDC42 inhibitor ML141 (100 μM) had the strongest inhibitory effects on the DOX-induced formation of nuclear γH2AX foci in all cell types under investigation (Fig. 2**a-c**). Inhibition of RAC1 GTPase-dependent signaling by EHop-016 (10 μM), EHT1864 (30 μM) and NSC23766 (100 μM) affected DOX-induced nuclear γH2AX foci formation only in H5V endothelial cells (Fig. 2**b**). Inhibition of RHOA GTPase by rhosin (100 μM) was ineffective in all cell types, whereas the RHO-kinase inhibitor Y-27632 (10 μM) reduced the number of DOX-induced nuclear γH2AX foci in both H5V endothelial cells and MEF but not in HL1 cardiomyocytes

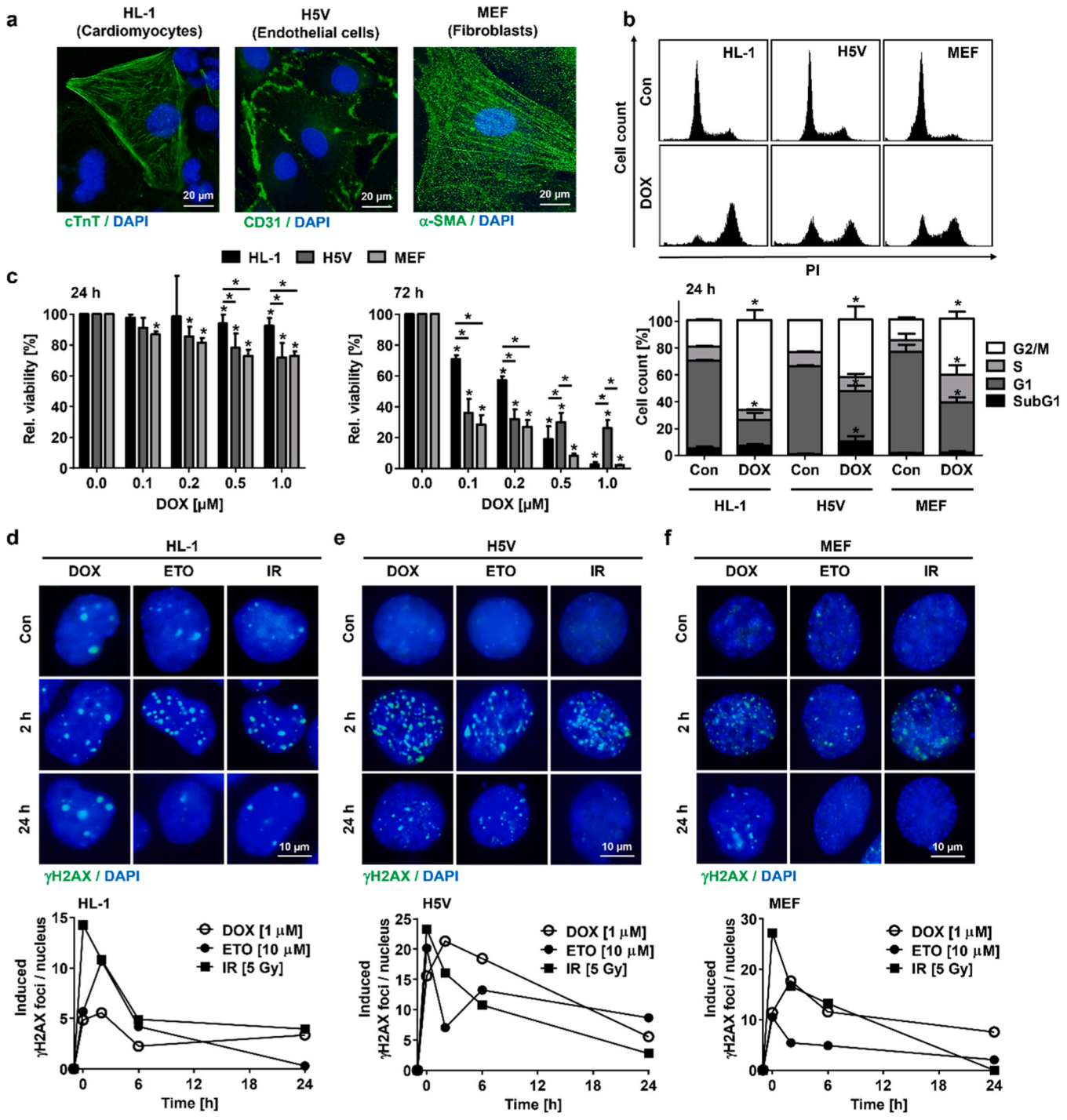

Fig. 1. DOX-induced cellular responses in established cardiac cell models. **a** Expression of cell type-specific markers was confirmed by immunocytochemistry in established cell lines (cTnT, HL-1 cardiomyocytes; CD31, H5V cardiac endothelial cells; α-SMA, MEF). Representative pictures show each cell type stained with the corresponding cell type-specific marker (green) and DAPI (blue); 100x objective. **b** Flow cytometric analysis of cell cycle distribution was performed after PI staining. Cells were pulse-treated with DOX for 2 h followed by a 24 h incubation period in the absence of the drug. Quantitative data shown in the histogram are the mean + SD from n=3–4 independent experiments. *p≤0.05 (vs. Con); one-way ANOVA, Bonferroni's post-hoc test. Representative results are shown in the upper part of the figure. **c** DOX-induced loss of cell viability was determined using the AlamarBlue™ assay after 24 h (left side) and 72 h (right side) treatment with increasing concentrations of DOX. Data shown are the mean + SD from n=3–6 independent experiments each performed in quadruplicates. *p≤0.05 (vs. Con); one-way ANOVA, Bonferroni's post-hoc test. **d-f** Cells were pulse-treated with 1 µM DOX or 1 µM ETO for 1 h or were irradiated with 5 Gy and post-incubated for 0.5 h. Analyses were performed after a post-incubation period of up to 24 h in drug-free medium. Induction (0 h) and repair of DSB (2–24 h) were monitored by immunofluorescent staining of nuclear γH2AX foci. Shown are representative pictures of DAPI (blue) stained nuclei with γH2AX foci (green); 100x objective. Quantitative data shown in the lower part are the mean from two independent experiments with >100 nuclei per condition being analyzed. Data obtained from additional extensive analyses are presented in **Supplementary Fig. 1**.

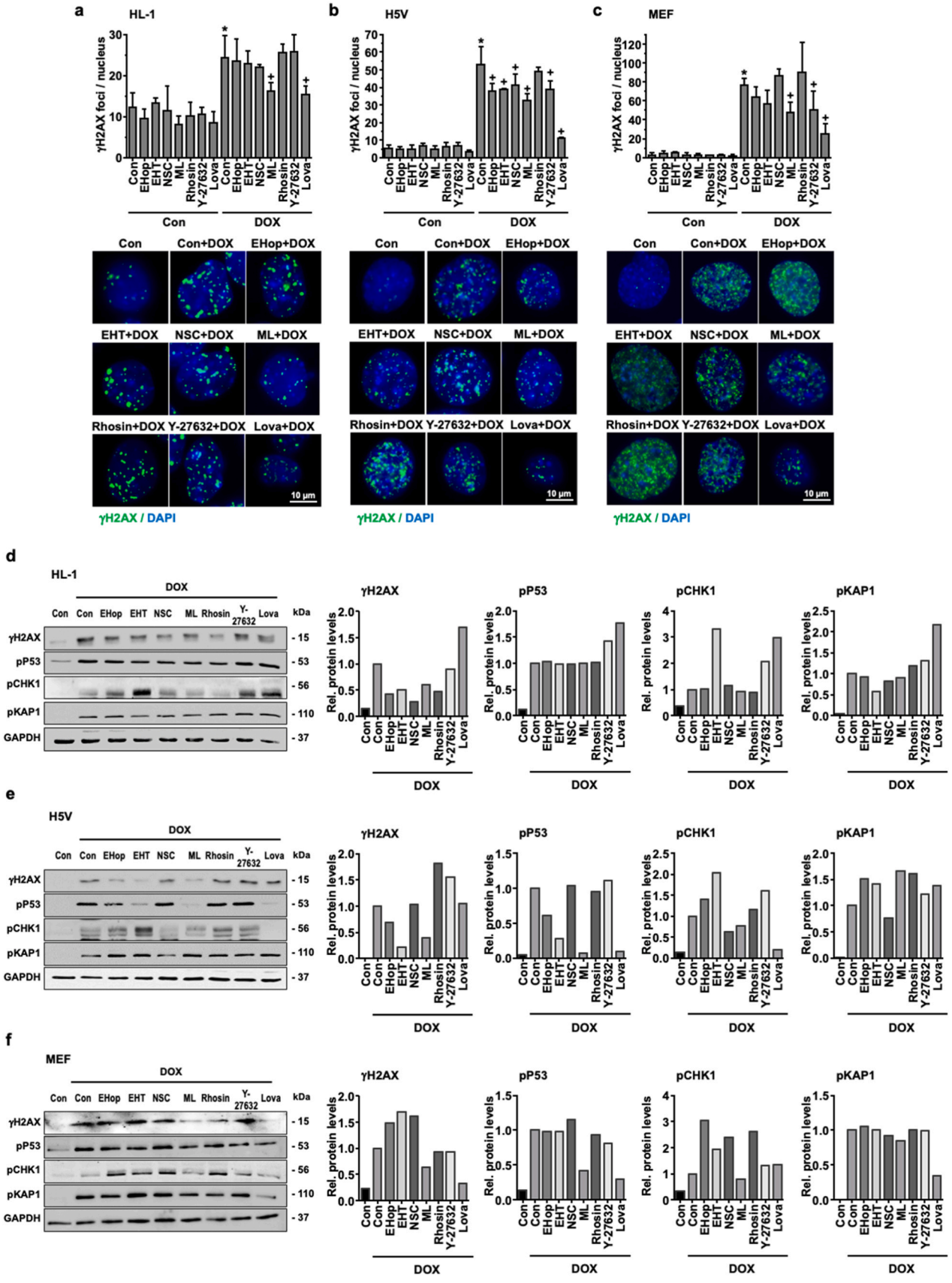

(caption on next page)

Fig. 2. Effect of RHO GTPase inhibitors on the DOX-induced formation of DSB and activation of DDR factors in established cardiac cell models. **a-c** Established cell lines were pre-treated with various RHO GTPase inhibitors (**Supplementary Table 1**) (10 μM EHop-016 (EHop), 30 μM EHT1864 (EHT), 100 μM NSC23766 (NSC), 100 μM ML141 (ML) 100 μM rhosin, 10 μM Y-27632 for 3 h or with 20 μM lovastatin (Lova), overnight), followed by 1 μM DOX co-treatment for 2 h. The number of nuclear γH2AX foci was quantified by immunocytochemistry. Quantitative data shown are the mean + SD from n=3–4 independent experiments with >50 nuclei per condition being analyzed. *p≤0.05 (vs. Con), $^{+}$p≤0.05 (vs. DOX); one-way ANOVA, Bonferroni's post-hoc test. The lower panels show representative pictures of DAPI (blue) stained nuclei with γH2AX foci (green) in each cell type after RHO GTPase inhibition and/or DOX treatment; 100x objective. For representative pictures of mono-treatment with inhibitors see **Supplementary Fig. 3**. **d-f** Cells were pre-treated with the RHO GTPase inhibitors as described above, followed by 1 μM DOX co-treatment for 2 h. Western blot analyses were performed using phospho-specific antibodies to detect the protein levels of γH2AX (S139), pP53 (S15), pCHK1 (S345) and pKAP1 (S824). Protein expression of GAPDH was used as loading control. After densitometrical analysis the signal intensity in DOX-treated samples was set to 1.0 and relative protein levels of the other experimental groups were shown as mean value from duplicate determinations. Representative pictures after mono-treatment with the inhibitors are shown in **Supplementary Fig. 7**.

(Fig. 2**a-c)**. Additional evaluation of DSB formation by the analysis of co-localized nuclear γH2AX/53BP1 foci showed similar results **(Supplementary Fig. 2b-d)**. Of note, mono-treatment with RHO inhibitors did not affect the basal number of DSB in any of the cell lines under investigation **(Supplementary Fig. 3)**. Summarizing, out of the three cardiac cell types tested, RHO GTPase inhibitors attenuated the formation of DSB by DOX treatment predominantly in H5V endothelial cells.

To gain deeper insight into the involvement of RHO GTPase-regulated functions in the regulation of DOX-induced mechanisms of the DDR, western blot analyses were performed. Using phospho-specific antibodies against representative DDR factors we found that DOX treatment increased the protein amounts of phosphorylated (activated) H2AX, P53, checkpoint kinase 1 (CHK1) and KRAB-associated protein 1 (KAP1) in all cell lines tested **(**Fig. 2**d-f)**. The pan-RHO GTPase inhibitor lovastatin attenuated the DOX-induced increase in γH2AX, pP53 and pKAP1 protein levels most clearly in MEF **(**Fig. 2**f)**, whereas in H5V endothelial cells DOX-induced pP53 and pCHK1 levels were preferentially lowered by lovastatin **(**Fig. 2**e)**. All RAC1 inhibitors (i.e., Ehop-016, ETH1864 and NSC23766), as well as the CDC42 inhibitor ML141 and RHOA inhibitor rhosin partially decreased the DOX-induced protein levels of γH2AX in HL-1 cells **(**Fig. 2**d)**. In H5V cells both EHT1864 and ML141 reduced DOX-stimulated γH2AX and pP53 protein levels **(**Fig. 2**e)**, while in MEF only ML141 led to a noticeable reduction in DOX-induced γH2AX and pP53 protein levels **(**Fig. 2**f).** Overall, comparing the inhibitory efficacy of different RHO GTPase inhibitors on DOX-simulated factors of the DDR between the different established cardiac cell lines, both the RAC1 inhibitor EHT1864 and the CDC42 inhibitor ML141 were most effective, especially in H5V endothelial cells.

To confirm the geno-protective effects observed after pharmacological inhibition of RAC1 and CDC42 in H5V endothelial cells, we additionally used an siRNA-based genetic approach to transiently knockdown Rac1 and Cdc42 expression, either alone or simultaneously **(Supplementary Fig. 4)**. Under our experimental setting, we achieved about 72% and 98% knockdown efficacy for RAC1 and CDC42 protein, respectively **(Supplementary Fig. 4a).** In line with pharmacological inhibition of RAC1 and CDC42, both siRac1 and siCdc42 moderately lowered the DOX-induced number of γH2AX foci in H5V cells **(Supplementary Fig. 4b)**. Simultaneous Rac1 and Cdc42 knockdown led to the strongest decrease in the DOX-induced γH2AX foci number **(Supplementary Fig. 4b)**. Consistent results were observed by western blot analysis detecting the DOX-induced activation of DDR-related proteins. SiRNA-based knockdown of Rac1 and Cdc42 partially reduced the DOX-induced protein levels of γH2AX, pP53, pCHK1 and pCHK2 **(Supplementary Fig. 4c)**. Simultaneous knockdown of both Rac1 and Cdc42 further reduced the protein levels, especially of γH2AX, pP53, pCHK1 and pKAP1, in DOX-treated cells **(Supplementary Fig. 4c)**. Hence, together with the inhibitor-based results, this genetic data supports the hypothesis that both RAC1 and CDC42 are involved in the regulation of DDR mechanisms in cardiac cell types treated with DOX **(Supplementary Fig. 4b-c)**.

Considering that oxidative damage is known to contribute to the pathogenesis of the DOX-induced cardiac injury [9,10] and RAC1 is involved in the ROS formation through NADPH oxidase [24], we assessed DOX-induced ROS levels and modulation of ROS formation by RAC1 inhibition in the different cardiac cell types **(Supplementary Fig. 5)**. Using low concentration of DOX (i.e. 1 μM), no notable increase in the ROS levels was found in any of the cell types as determined by the DCFDA assay **(Supplementary Fig. 5)**. This data indicate that ROS formation is not of major relevance for the effects we observed under our experimental conditions (i.e., low DOX concentrations). At high concentration of DOX (10 μM) a moderate increase in ROS levels was detectable in both HL-1 cardiomyocytes and MEF, but not in H5V endothelial cells **(Supplementary Fig. 5)**. Of note, RAC1 inhibition by EHT1864 preferentially decreased ROS levels induced by 10 μM DOX in MEF **(Supplementary Fig. 5)**, supporting the hypothesis that RAC1 is involved in ROS production when high DOX concentrations are applied [43].

3.3. DOX-induced cytotoxicity and DDR in primary murine cardiac cells in vitro

In the next step we employed primary cardiac cells isolated from the hearts of adult C57BL/6 mice to corroborate the results obtained from the use of the established cell lines. Immunocytochemical analyses confirmed that the primary cardiac cells express the cell type-specific markers (i.e., cardiomyocytes, cTnI; endothelial cells, CD31; fibroblasts, α-SMA) as anticipated (Fig. 3**a)**. Analysis of cell viability showed moderate differences in the DOX sensitivity between the different primary cardiac cell types **(**Fig. 3**b).** The obtained IC_{50} values indicate that primary cardiac endothelial cells are slightly more resistant to high DOX concentrations (IC_{50}: >5 μM) than primary cardiomyocytes and cardiac fibroblasts (IC_{50}: ~2.5 μM each) **(**Fig. 3**b)**. Apoptosis frequency as determined by the TUNEL assay revealed a high percentage of TUNEL positive cardiomyocytes (~20%) already under basal conditions, while endothelial cells and fibroblasts showed a comparably low number (i.e. <5%) of apoptotic cells **(**Fig. 3**c)**. Most important, a significant increase in DOX-stimulated apoptosis frequency was detected in primary endothelial cells and fibroblasts but not in primary cardiomyocytes **(**Fig. 3**c)**. Furthermore, DOX treatment caused only a minor increase in DSB levels, as reflected by nuclear γH2AX foci, in primary cardiomyocytes **(**Fig. 3**d)**. This is fully consistent with the results observed with the established cardiomyocyte cell line **(**Fig. 1**d and Supplementary Fig. 2a)**. Noteworthy, primary cardiac endothelial cells and fibroblasts exhibited an approximately 2- and 4-fold stronger increase in the number of nuclear γH2AX foci after DOX treatment than cardiomyocytes **(**Fig. 3**d)**. Moreover, only primary endothelial cells and fibroblasts showed a marked decline in the number of γH2AX foci over a post-treatment period of 24 h, which is indicative of efficient DSB repair. By contrast, the number of nuclear γH2AX foci remained largely unchanged over time in primary cardiomyocytes **(**Fig. 3**d)**. Overall, the data show that primary cardiomyocytes are characterized by the generation of lower numbers of DSB following DOX exposure and a less efficient DSB repair as compared to primary non-cardiomyocytes (i.e., cardiac endothelial cells and cardiac fibroblasts).

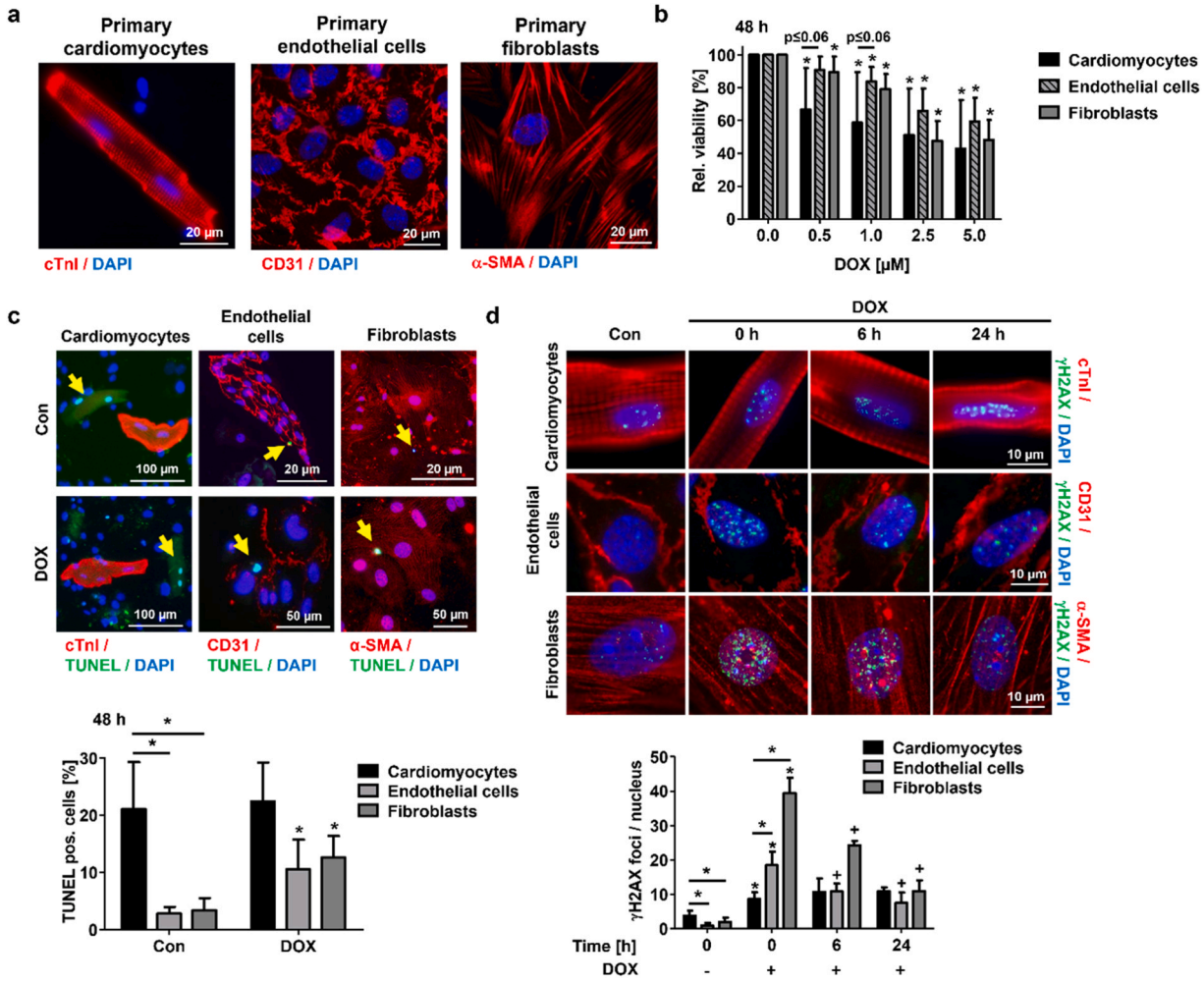

Fig. 3. DOX-induced cytotoxicity and DSB formation in primary cardiac cell types. **a** Primary cardiac cells were isolated from the hearts of C57BL/6 mice as described in methods. Cell type-specific markers were used to confirm the successful isolation of the different cardiac cell types (cTnI, cardiomyocytes; CD31, endothelial cells; α-SMA, fibroblasts). Representative pictures show each cell type stained with the corresponding cell type-specific marker (red), DAPI (blue); 100x objective. **b** AlamarBlue™ assay was performed to assess the viability of primary cardiac cells 48 h after treatment with increasing concentrations of DOX. Data shown are the mean + SD from n=6–12 independent experiments, each performed in biological triplicates. *p≤0.05 (vs. Con), ns, not significant; one-way ANOVA, Bonferroni's post-hoc test. **c** Cells were treated with 1 µM DOX for 48 h and the percentage of apoptotic cells was determined by the TUNEL assay. Data shown are the mean + SD from n=3–8 independent experiments. *p≤0.05 (vs. Con); one-way ANOVA, Bonferroni's post-hoc test. The upper panel shows representative pictures of each cell type stained with the corresponding cell type-specific marker (red), TUNEL (green), DAPI (blue); 20x objective. TUNEL positive cells are exemplarily indicated by yellow arrows. **d** To analyze DOX-induced DSB formation and repair, cells were pulse-treated with 1 µM DOX for 2 h and further incubated up to 24 h in the absence of DOX. The number of nuclear γH2AX foci was quantified by immunocytochemistry. Data shown in the histogram (lower panel) are the mean + SD from n=3–11 independent experiments with >50 nuclei per condition being analyzed. *p≤0.05 (vs. 0 h Con), $^{+}$p≤0.05 (vs. 0 h DOX), ns, not significant; one-way ANOVA, Bonferroni's post-hoc test. The upper panel shows representative pictures of each cell type stained with the corresponding cell type-specific marker (red), γH2AX (green), DAPI (blue); 100x objective.

3.4. Influence of pharmacological inhibition of RHO GTPase-regulated signaling pathways on DOX-induced stress responses of primary cardiac cell types in vitro

Analyzing the effect of pharmacological inhibitors of RHO GTPase-regulated signaling on the formation of nuclear γH2AX foci after DOX exposure in primary cardiac cells, we found that the RAC1 inhibitor EHT1864, the CDC42 inhibitor ML141 and the dual RAC1/CDC42 inhibitor Aza1 confer the strongest protection from DOX-induced DSB formation in all primary cardiac cell types tested, whereas rhosin and lovastatin were only poorly effective under our experimental setting (Fig. 4**a-c**).

Next, we investigated the influence of RAC1-regulated signaling on the repair of DOX-induced DSB by comparatively monitoring the time-dependent decline of nuclear γH2AX foci in the presence or absence of the RAC1 inhibitor EHT1864. In these analyses we focused on RAC1 having in mind that targeting of RAC1 signaling has been repeatedly demonstrated to protect against DOX-induced geno- and cytotoxicity both in vitro and in vivo [19,22,23,34]. EHT1864 significantly reduced the DOX-induced formation of γH2AX foci at early time point (i.e., after 2 h of DOX treatment) in all examined cardiac cell types (Fig. 4**d-f**), whereas the number of residual γH2AX foci (i.e., 24 h post-treatment period) remained unaffected by EHT1864 in endothelial cells and fibroblasts (Figs. 4**e and** 4**f**). In cardiomyocytes, the residual number of DOX-induced γH2AX foci was significantly reduced by EHT1864 pre-treatment (Fig. 4**d**), indicating that inhibition of RAC1-related signaling specifically decreases the level of persistent DNA damage in cardiomyocytes.

To further characterize the involvement of RAC1 in the regulation of the cell type-specific responsiveness to DOX, the level of phosphorylated (activated) DDR-related factors was analyzed by western blot analyses in the presence and absence of the RAC1 inhibitor EHT1864. DOX

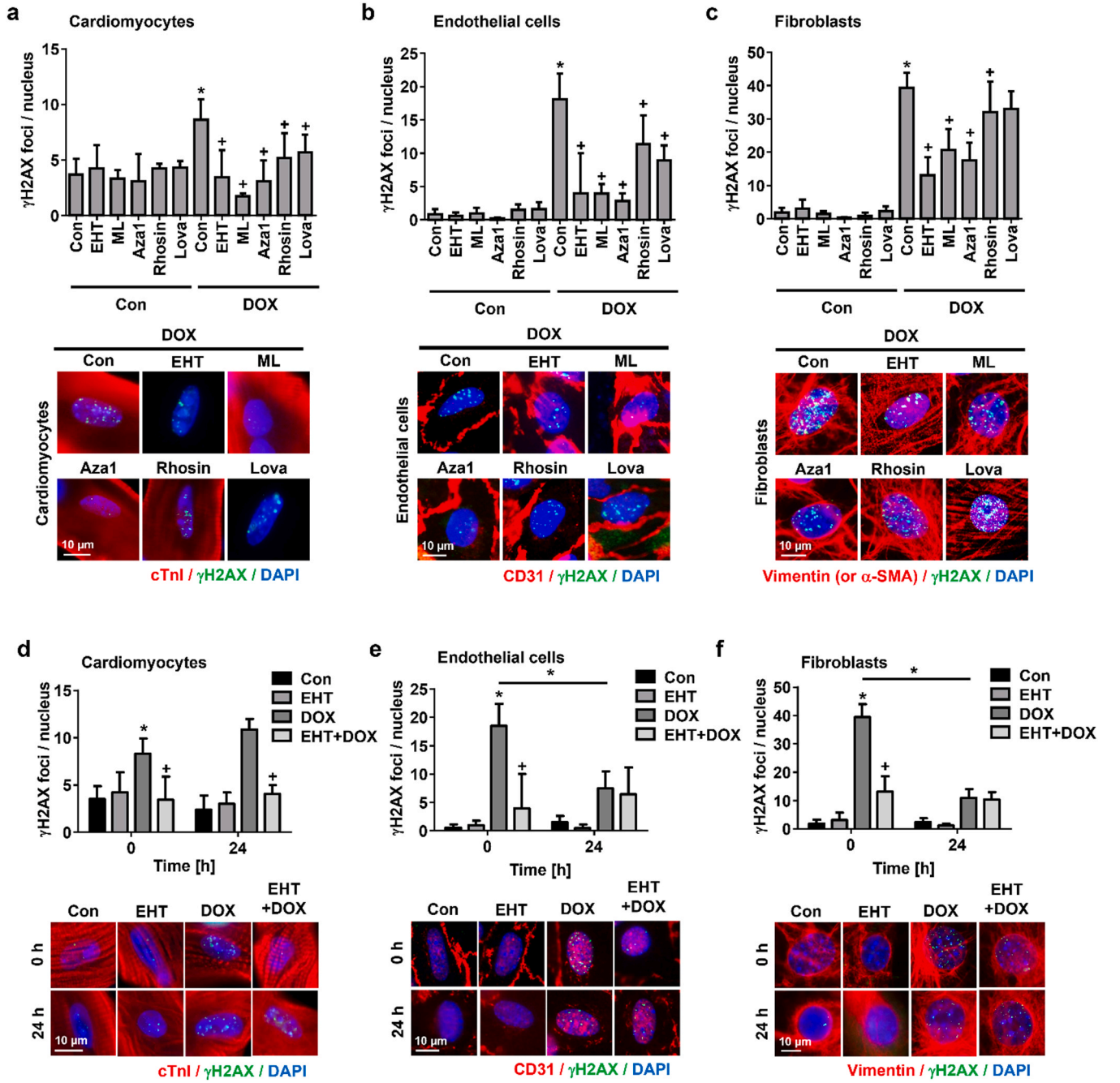

Fig. 4. Effect of RHO GTPase inhibitors on DOX-induced DSB formation and repair in primary cardiac cells. **a-c** Primary cardiac cell types were pre-treated with different RHO GTPase inhibitors (**Supplementary Table 1**) (30 µM EHT1864 (EHT), 100 µM ML141 (ML) , 10 µM Aza1, 100 µM rhosin for 3 h or with 20 µM lovastatin (Lova), overnight), followed by 1 µM DOX co-treatment for 2 h. The number of DOX-induced γH2AX foci in the presence or absence of RHO GTPase inhibitors was quantified. Data shown are the mean + SD from n=3–11 independent experiments with >50 nuclei per condition being analyzed. *p≤0.05 (vs. Con), $^{+}$p≤0.05 (vs. DOX); one-way ANOVA, Bonferroni's post-hoc test. The lower panels show representative pictures of each cell type stained with the corresponding cell type-specific marker (red), γH2AX (green), DAPI (blue); 100x objective. Control pictures of mono-treatment with RHO GTPase inhibitors treated cells are shown in **Supplementary Fig. 6**. **d-f** Primary cardiac cells were pre-treated with 30 µM EHT for 3 h, followed by 1 µM DOX co-treatment for 2 h. To evaluate DSB induction and repair, the number of nuclear γH2AX foci was quantified by immunocytochemistry immediately after the DOX pulse-treatment (0 h) or after post-incubation (24 h), respectively, in the absence of EHT and DOX. Data shown are the mean + SD from n=3–11 independent experiments with >50 nuclei per condition being analyzed. *p≤0.05 (vs. corresponding Con), $^{+}$p≤0.05 (vs. corresponding DOX); one-way ANOVA, Bonferroni's post-hoc test. The lower panels show representative pictures of each cell type stained with the corresponding cell type-specific marker (red), γH2AX (green), DAPI (blue); 100x objective.

treatment induced a strong activation of DDR-related factors in endothelial cells and fibroblasts, but not in cardiomyocytes (except for pKAP1) as concluded from the elevated protein levels of γH2AX, pP53 and pKAP1 in DOX treated cells as compared to untreated controls (Fig. 5**a-c**). Consistent with the results obtained from the immunocytochemical γH2AX foci analysis, the DOX-induced increase in the protein levels of the aforementioned phosphorylated DDR-related factors were significantly attenuated by EHT1864 in primary cardiac endothelial cells and fibroblasts (Fig. 5**b-c**). In addition, EHT1864 inhibited DOX-induced increase of pKAP1 in cardiomyocytes **(Fig, 5a)** and lowered the level of pCHK2 in DOX-treated fibroblasts (Fig. 5**c**).

To investigate the influence of RAC1 inhibition by EHT1864 on the

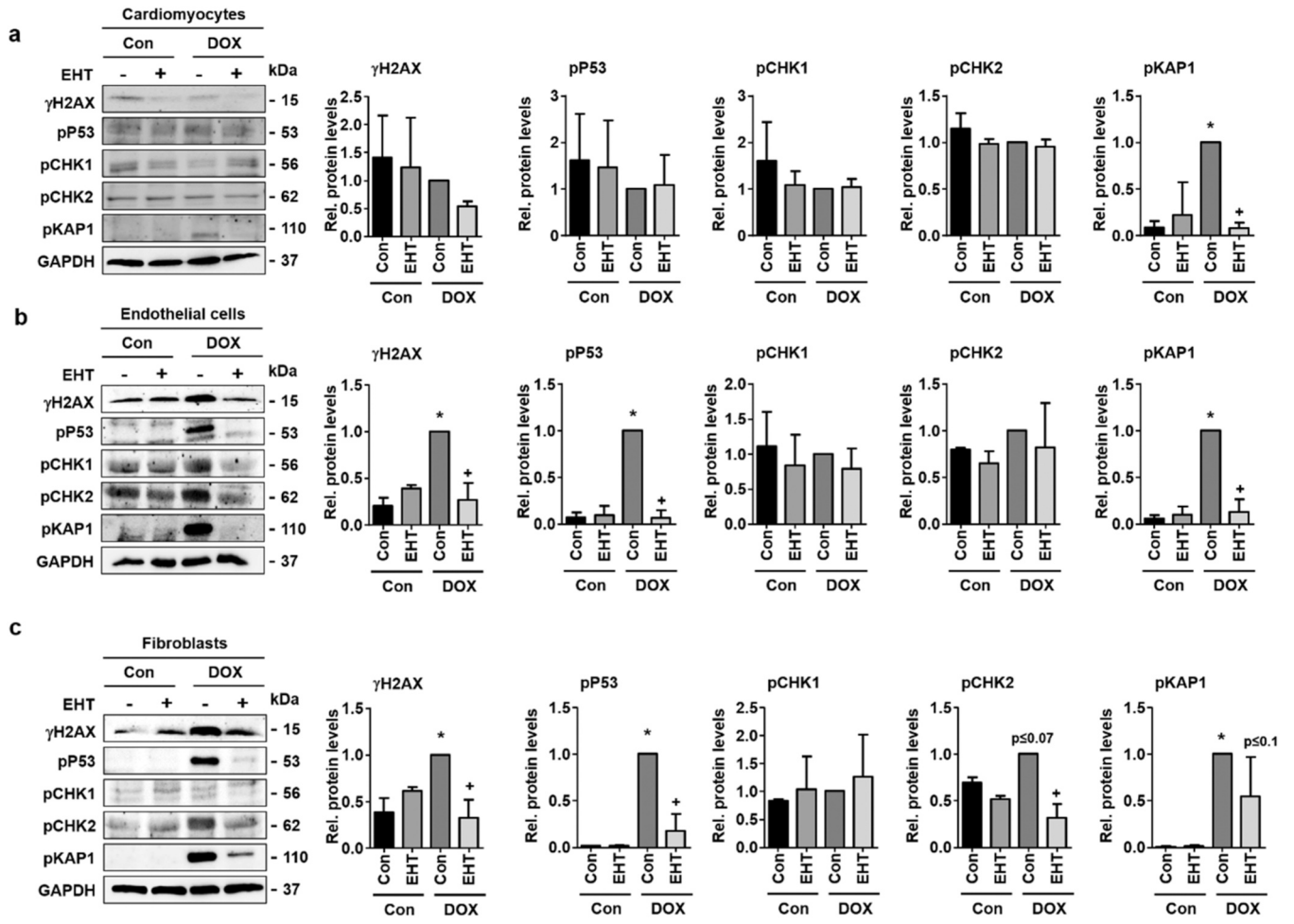

Fig. 5. Effect of RHO GTPase inhibitors on DOX-induced DDR activation in primary cardiac cells. **a-c** Primary cardiac cells were pre-treated with 30 μM EHT for 3 h, followed by 1 μM DOX co-treatment for 2 h. Western blot analyses were performed using phospho-specific antibodies to detect the protein levels of γH2AX (S139), pP53 (S15), pCHK1 (S345), pCHK2 (T68) and pKAP1 (S824). Protein expression of GAPDH was used as loading control. After densitometrical analysis the signal intensity of DOX-treated samples was set to 1.0 and relative protein levels of the other experimental groups were shown as mean + SD from n=3 independent experiments (primary cardiac cell types isolated from 3 individual animals). *p≤0.05 (vs. Con), $^{+}$p≤0.05 (vs. DOX); one-way ANOVA, Bonferroni's post-hoc test. Representative blots are shown on the left side.

cytotoxicity resulting from DOX exposure, cell viability and apoptosis were monitored. We observed that EHT1864 does not protect primary cardiac cells from DOX-induced loss of viability (Fig. 6**a-c**). Moreover, EHT1864 mono-treatment caused a significant increase of TUNEL-positive endothelial cells and fibroblasts (Fig. 6**d**), indicating that inhibition of RAC1 is sufficient to promote pro-apoptotic pathways in these cardiac cell types. Taken together, the substantial protection of cardiac cells from DOX-induced DNA damage formation by EHT1864 (Fig. 4**d-f**) did not manifest in relation to DOX-induced cytotoxicity, very likely due to the stimulation of pro-apoptotic pathways by EHT1864 mono-treatment, which however appears to occur in a DNA-damage independent manner (Fig. 6**d**).

3.5. DOX-induced DNA damage formation in different cardiac cell types and the influence of RHO GTPases in vivo

In extension of our in vitro data, we employed a mouse model to monitor the in vivo effects of DOX treatment and pharmacological inhibition of RHO GTPases on the formation of DNA damage in different cardiac cell populations. For this purpose, heart tissue sections were analyzed, which were obtained from mice treated with multiple doses of DOX (6 ×3 mg/kg BW) over several weeks ± pan-RHO GTPase inhibitor (lovastatin) or RAC1 inhibitor (NSC23766) [34]. The heart sections were stained with Alexa Fluor™-conjugated WGA to allow morphological discrimination between cardiomyocytes and non-cardiomyocytes. We observed that the percentage of γH2AX positive cardiomyocytes was relatively high (~15%) in saline-treated control animals as compared to non-cardiomyocytes (<5%) (Figs. 7**a and** 7**b**). DOX treatment led to a significant increase in the percentage of both cardiomyocytes and non-cardiomyocytes harboring DNA damage, which was significantly reduced by both lovastatin and NSC23766 co-treatment in both cardiac cell types (Figs. 7**a and** 7**b**). The results of the in vivo studies further support the hypothesis that both cardiomyocytes and non-cardiomyocytes are susceptible to DNA damage formation following DOX treatment in vivo and, furthermore, that signaling mechanisms regulated as a function of RHO GTPases, especially RAC1, influence the level of DOX-induced residual DNA damage in both cardiac cell populations.

4. Discussion

Anthracycline-induced cardiotoxicity is a multifaceted process and emerges from diverse inter- and intracellular responses of cardiac tissue [1,2]. Anthracyclines induce DNA damage by different mode of action, thereby activating the complex network of the DDR, which defines the balance between cell survival and death [3] and also influences

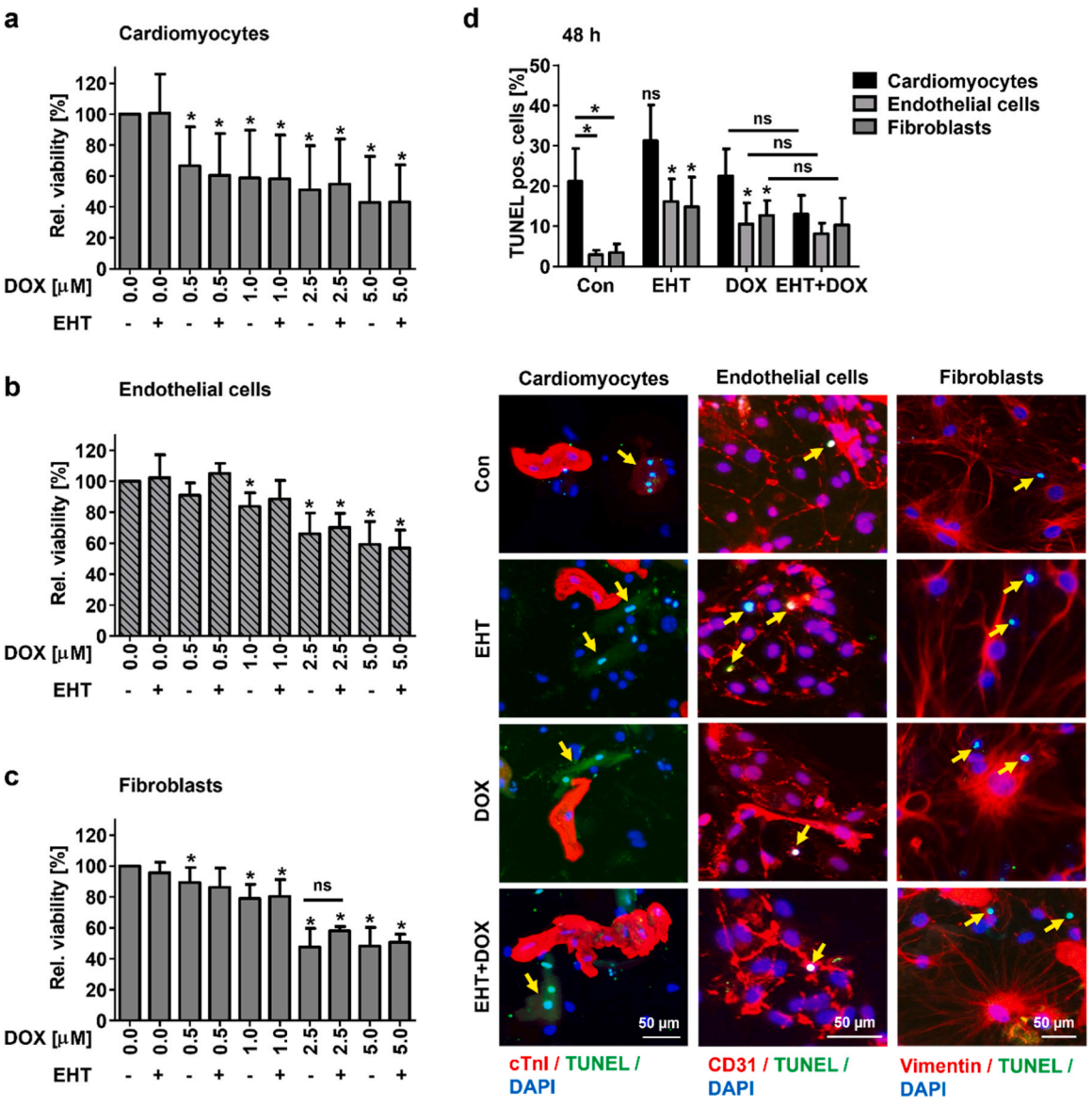

Fig. 6. Effect of RAC1 inhibition on DOX-induced cytotoxicity in primary cardiac cells. **a-c** Primary cardiac cells were treated with 30 µM EHT1864 (EHT) for 3 h, followed by treatment with increasing concentrations of DOX for 48 h in the absence of EHT. AlamarBlue™ assay was performed to assess the DOX-induced loss of cell viability following RAC1 inhibition. Data shown are the mean + SD from n=3–12 independent experiments each performed in biological triplicates. *p≤0.05 (vs. corresponding Con); one-way ANOVA, Bonferroni's post-hoc test. **d** Primary cardiac cells were treated with 30 µM EHT1864 (EHT) for 3 h, followed by 1 µM DOX treatment for 48 h in the absence of EHT. Immunocytochemical TUNEL assay was performed to quantify the percentage of apoptotic cells. Data shown are the mean + SD from n=3–8 independent experiments. *p≤0.05 (vs. Con), ns, not significant; one-way ANOVA, Bonferroni's post-hoc test. The lower panel shows representative pictures of each cell type stained with the corresponding cell type-specific marker (red), TUNEL (green), DAPI (blue); 20x objective. TUNEL positive cells are exemplarily indicated by yellow arrows.

DOX-induced cardiotoxicity [44]. Although cardiomyocytes constitute the largest part of the heart, they are outnumbered by non-cardiomyocytes, which possess crucial functions in the maintenance of cardiac homeostasis [45]. Hence, we hypothesize that different cardiac cell types contribute to cardiac damage evoked by anthracyclines with multiple RHO GTPase-regulated signaling pathways being involved. To test this hypothesis, we employed both established and primary cardiac cell models and investigated their response to DOX-induced cellular stress and the impact of RHO GTPases on this response. We observed that DOX-induced cell death, activation of cell cycle checkpoints, as well as formation and repair of DSB considerably varied in a cell type-dependent manner. DOX induced very low levels of DSB in both established HL-1 cardiomyocytes and primary cardiomyocytes. By contrast, a robust induction of DSB was detected in both established and primary non-cardiomyocytes (i.e., endothelial cells and fibroblasts). This supports the hypothesis that non-cardiomyocyte cell types of the heart are of additional relevance for the pathophysiology of DOX-induced cardiotoxicity [44,46]. This is in line with previous reports suggesting that, besides cardiomyocytes, cardiac endothelial cells, cardiac fibroblasts, and cardiac progenitor cells also contribute to cardiotoxicity evoked by anthracycline exposure [44]. Of note, both HL-1 and primary cardiomyocytes failed to repair DOX-induced DSB, whereas primary non-cardiomyocytes showed efficient DSB repair activity. Since HL-1 cardiomyocytes showed an efficient repair of DSB that were induced by IR or the TOP2 inhibitor ETO, we speculate that the relatively low levels of DSB induced by DOX are not sufficient to activate the DSB repair machinery in cardiomyocytes [47]. Alternatively, cardiomyocytes may suffer from a specific deficit in the processing of DSB induced by anthracyclines. Overall, our findings demonstrate that cardiomyocytes are least responsive to DSB induction

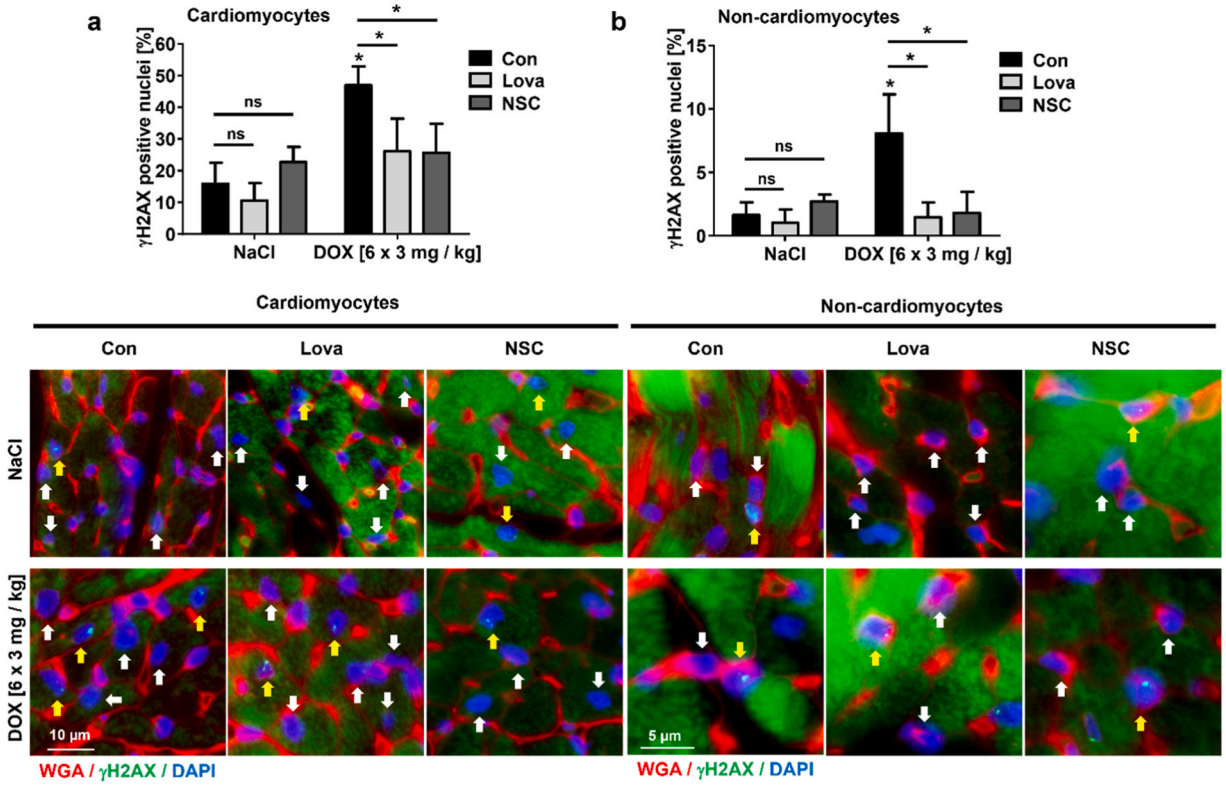

Fig. 7. Comparative analysis of the impact of RHO GTPase inhibitors on DOX-induced increase in residual DSB in cardiomyocytes and non-cardiomyocytes, following DOX treatment in vivo. **a, b** 8–10 weeks old C57BL/6 mice were treated with lovastatin (Lova) (10 mg/kg BW, p.o.) or the RAC1 inhibitor NSC23766 (NSC) (5 mg/kg BW, i.p.) three times a week. Multiple doses of DOX (6 ×3 mg/kg BW, i.p.) were administered to the mice and 6 days after the last DOX injection hearts were isolated for analyses [34]. Formalin-fixed paraffin-embedded heart tissue sections were stained with WGA to visualize cell borders. The proportion of γH2AX positive cardiomyocytes (a) and non-cardiomyocytes (b) were quantified. Data shown are the mean from 3 animals being analyzed per experimental group with >150 nuclei per condition being analyzed. *p≤0.05 (vs. corresponding Con), ns, not significant; one-way ANOVA, Bonferroni's post-hoc test. The lower panels show representative pictures of heart sections stained with WGA (red), γH2AX (green), DAPI (blue); 100x objective. White arrows indicate cardiomyocytes or non-cardiomyocytes in each corresponding panel and yellow arrows exemplarily indicate γH2AX positive cells.

by DOX and harbor the lowest DSB repair capacity at the same time. Notably in this context, we did not observe an increase in ROS levels following treatment with clinically relevant low concentration of DOX (i.e., 1 μM), indicating that oxidative damage may not be of major relevance for the effects observed under our experimental conditions [43].

Regarding the involvement of RHO GTPase-regulated signaling in DOX-induced stress responses in different cardiac cell types, we observed that inhibition of various RHO GTPases significantly reduced the formation of DSB following DOX exposure. We found a preferential inhibitory effect of RAC1 inhibitors (i.e., EHop-016, EHT1864 and NSC23766) on DOX-induced DSB formation in H5V cardiac endothelial cells, while the pan-RHO GTPase inhibitor lovastatin and the CDC42 inhibitor ML141 were effective in all established cardiac cell types. Lovastatin was less effective in primary cardiac cells as compared to established cell lines. We speculate that this might be related to different expression and/or activity of various RHO GTPases in established versus primary cardiac cell models. Moreover, specific inhibition of either RAC1 (by EHT1864) or CDC42 (by ML141) or simultaneous inhibition of both RHO GTPases (by Aza1) significantly lowered the DOX-induced formation of DSB in all primary cardiac cells. Noteworthy, siRNA-based simultaneous knockdown of Rac1 and Cdc42 clearly lowered the DOX-induced formation of DSB and the activation of selected DDR factors in H5V endothelial cells, supporting the results obtained from the inhibitor-based studies. Overall, there are substantial differences between established and primary cardiac cells with regard to their responsiveness to RHO inhibition. In this context it is also worthwhile to note that the RHOA inhibitor rhosin protected each of the primary cardiac cell types from DOX-induced DNA damage, but none of the established cell lines. However, the effect of rhosin was less pronounced as compared to that of the RAC1 and CDC42 specific inhibitors. Altogether, these findings indicate that RAC1- and CDC42-regulated signaling probably plays a central role in the formation of DOX-induced DSB in cardiac cells. Furthermore, inhibition of RAC1-dependent mechanisms affects the levels of residual DNA damage in a cell type-specific manner in vitro. To date, inhibition of RAC1 signaling has been suggested to be of particular relevance for the protection of the heart against anthracycline-induced cardiac damage [19,20,23,33,34,36]. The data presented in this study provide novel evidence that, in addition to RAC1, CDC42-regulated mechanisms also substantially influence the extent of cardiac damage evoked by DOX treatment. This is meaningful for forthcoming in vitro and in vivo studies aiming to develop novel cardioprotective measures in the context of DOX-based anticancer therapy.

Assuming that DOX-induced DNA damage that triggers the subsequent activation of the DDR contributes to the pathophysiology of anthracycline-mediated cardiotoxicity, the question arises as to which molecular mechanism of the highly complex DDR might be of particular relevance. To this end, we characterized the influence of RHO GTPase inhibitors on DOX-induced activation of prototypical DDR factors [48]. Summarizing the complex set of data obtained from extensive western blot-based analyses employing different established and primary cardiac cell types and various RHO GTPase inhibitors, we hypothesize that inhibition of DOX-induced functions regulated especially by P53 and KAP1 are of utmost relevance for the genoprotective effects mediated by RHO GTPase inhibitors. In line with this hypothesis, P53-regulated

mechanisms are reported to influence DOX-induced cardiotoxicity [20]. We speculate that the variable efficacy of the diverse RHO GTPase inhibitors on DOX-stimulated DDR mechanisms observed in different cardiac cell types is due to differences in the expression level and/or activity of RHO GTPases, RHO-regulatory factors (i.e., guanine nucleotide exchange factors (GEF) and/or GTPase activating proteins (GAP)), TOP2 isoforms, TOP2-regulatory proteins as well as DDR- and DNA repair-related factors. Deciphering the high complexity of these potentially influencing factors will be subject of future cardio-oncological studies aiming to develop effective cardioprotective measures.

P53 plays a well-recognized key role in the regulation of DNA repair as well as of cell survival and death pathways [49]. Bearing in mind that DOX-induced DNA damage triggers the activation of P53-regulated mechanisms, and this response can be modulated by RHO GTPase inhibitors, it is feasible that P53-related signaling determines the fate of cardiac cell types after DOX exposure. Investigating the influence of DOX on viability and apoptosis of primary cardiac cell types, we observed a high apoptosis frequency in primary cardiomyocytes already under basal conditions, which is presumably due to the fragility of primary cardiomyocytes in culture [40]. Yet, 48 h of DOX treatment did not trigger any further increase in apoptotic fraction of primary cardiomyocytes. By contrast, primary cardiac endothelial cells and fibroblasts showed relatively low basal frequency of apoptotic cells, which however was significantly increased after DOX treatment. Accordingly, we detected DOX-induced increase in P53 phosphorylation only in primary cardiac endothelial cells fibroblasts, but not in primary cardiomyocytes. Noteworthy in this context, adult cardiomyocytes can develop resistance to intrinsic apoptosis [50]. Furthermore, it was shown that DOX stimulates either apoptosis or senescence in neonatal cardiomyocytes depending on the DOX dose applied [51]. Hence, we speculate that the relevant DNA damage-related toxicity pathways (e.g., apoptosis or senescence) and cardiac cell types involved are depending on both the maturity of the cardiac cell types (i.e., adult or neonatal stage), the DOX dose administered, the time point of analysis as well as the treatment regimen used (acute or subacute treatment) [37].

Unexpectedly, we found that not only DOX, but also EHT1864 treatment significantly stimulated apoptosis in primary non-cardiomyocytes. This indicates that RAC1 regulates mechanisms that protect non-cardiomyocytes from undergoing apoptosis under non-stressed conditions [52]. Of note, this pro-apoptotic effect of EHT1864 is independent of DNA damage formation as concluded from the results obtained from nuclear γH2AX foci and western blot analyses. In line with our data, promotion of apoptosis by EHT1864 was also reported by others [53]. We speculate that the observed pro-apoptotic effect of EHT1864 is related to the well-known role of RAC1 as a key regulator of apoptosis-related pathways, including NF-κB and MAPK signaling [25,26]. Accordingly, under the situation of co-treatment with DOX, EHT1864 did not significantly protect primary cardiac cells from DOX-induced apoptosis. We assume that the geno-protective effect of EHT1864 as demonstrated by the profound attenuation of DOX-induced DSB formation and reduced activation of DDR factors is not reflected on the level of apoptosis because of simultaneous activation of DNA damage-independent pro-apoptotic pathways under our experimental setting. Having in mind that additional cell death pathways (e.g., autophagy, ferroptosis, pyroptosis) contribute to DOX-induced cardiotoxicity [37], it remains feasible that RHO GTPase-signaling interferes with such alternative cell death-related mechanisms [54,55].

Apart from the regulation of apoptosis, P53 is also a well-known regulator of senescence [56]. Noteworthy in this context, persistent DNA damage, which can be triggered by endogenous or exogenous noxae, is associated with a premature senescence-associated phenotype in adult cardiomyocytes [57,58]. Moreover, DOX can induce accelerated cardiomyocyte senescence, eventually contributing to late-onset cardiotoxicity [51,59,60]. In line with these reports, we observed a high percentage of γH2AX positive cardiomyocytes (~15%) already under basal conditions in vivo and a prolonged persistence of DNA damage evoked by DOX in cardiomyocytes in vitro. Hence, we assume that DOX exposure evokes senescence-associated DNA damage formation in cardiomyocytes. Moreover, our results demonstrated that pharmacological inhibition of RHO GTPases, especially of RAC1, protected not only cardiomyocytes but also non-cardiomyocytes from DOX-induced increase in residual DSB in vivo. Of note, this geno-protective effect resulting from RAC1 inhibition was observed in a subacute setting, where repeated low dose of DOX was administered and analysis was performed at a late time point. In line with this, we previously showed that cardiomyocyte-specific Rac1 deletion provides a partial protection against DOX-induced cardiac damage specifically in a subacute setting [36]. Noteworthy, such subacute treatment scheme better reflects the clinically relevant anticancer treatment regimen than the frequently used acute models. Hence, assessing the potential cardioprotective efficacy resulting from RHO GTPase inhibition in the context of DOX-based anticancer therapy, it is important to consider that the adverse cardiac outcome pathways triggered by DOX treatment in vivo are likely both dose and time dependent [51]. Collectively, the available data suggest that inhibition of RHO GTPases, especially of RAC1, may be clinically useful to protect cardiac cells from persistent DNA damage that is formed as a result of repeated DOX exposure and eventually triggers senescence [57–60].

Taken together, the results of our study support the model **(**Fig. 8**)** that, in addition to cardiomyocytes, cardiac endothelial cells and fibroblasts also contribute to the irreversible cardiotoxicity evoked by DOX treatment, with both RAC1- and CDC42-regulated signaling pathways being of pathophysiological relevance. We assume that signaling pathways regulated by these RHO GTPases promote the formation of DNA damage (i.e., low DNA damage in cardiomyocytes and robust DNA damage in non-cardiomyocytes) and subsequent activation of DDR-related mechanisms following DOX treatment. Therefore, we suggest simultaneous pharmacological targeting of RAC1- and CDC42-regulated pathways in multiple cardiac cell types as the most promising approach to mitigate detrimental late-onset adverse effects on the heart evoked by anthracycline-based anticancer therapy.

Ethics approval

Animal experiments were conducted in accordance with the European Guidelines for the Care and Use of Laboratory Animals (2010/63/EU) and were approved by the North Rhine-Westphalia State Agency for Nature, Environment and Consumer Protection (approval reference number: 84–02–04.2011.A183).

Funding

This study was supported by Deutsche Krebshilfe (70113753) and the Deutsche Forschungsgemeinschaft (DFG; FR 1241/16-1).

CRediT authorship contribution statement

Lena Abbey: Investigation, Visualization. **Pelin Kücük:** Formal analysis, Investigation, Methodology, Validation, Visualization, Writing – original draft, Writing – review & editing. **Gerhard Fritz:** Conceptualization, Formal analysis, Funding acquisition, Project administration, Resources, Supervision, Writing – original draft, Writing – review & editing. **Christian Henninger:** Formal analysis, Supervision, Writing – original draft. **Joachim Schmitt:** Methodology.

Declaration of Competing Interest

The authors declare the following financial interests/personal relationships which may be considered as potential competing interests Gerhard Fritz reports financial support was provided by German Cancer Aid and the Deutsche Forschungsgemeinschaft (DFG). If there are other authors, they declare that they have no known competing financial

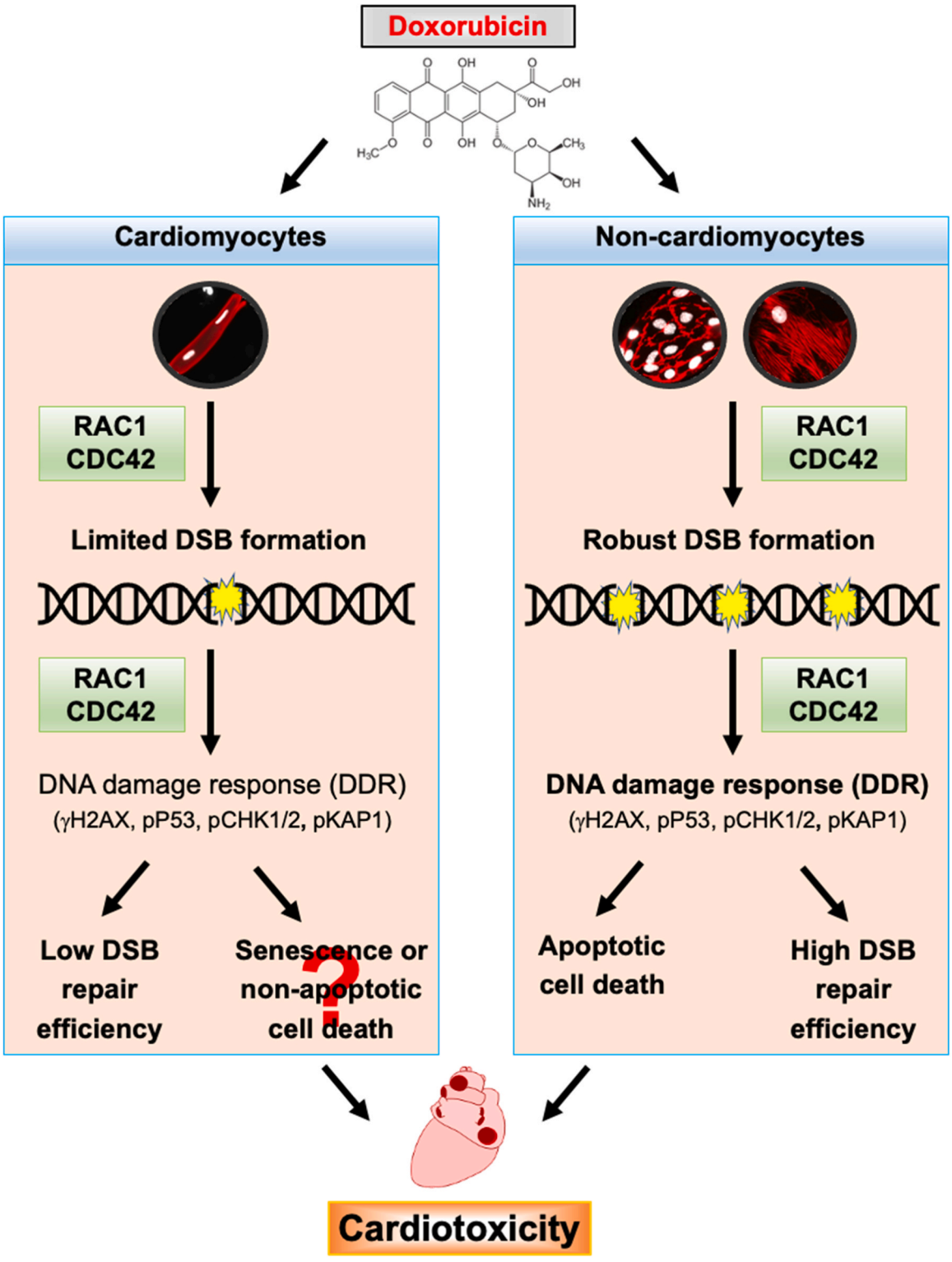

Fig. 8. Hypothetical model of the contribution of various cardiac cell types and RHO GTPases in DOX-induced cardiac injury. We hypothesize that DOX impacts both cardiomyocyte (low initial DNA damage formation) and non-cardiomyocyte populations (robust initial DNA damage formation) of the heart with RAC1- and CDC42-regulated pathways contributing to DSB formation and DDR activation, leading to cell type-specific cellular responses eventually triggering cardiotoxicity.

interests or personal relationships that could have appeared to influence the work reported in this paper.

Data Availability

No data was used for the research described in the article.

Acknowledgements

We would like to thank Claudia Gavranic (Institute of Toxicology) and Annika Zimmermann (Institute of Pharmacology) for excellent technical support. Furthermore, we thank Dr. Jan Ohlig (HHU, Düsseldorf) for providing the heart tissue sections.

Appendix A. Supporting information

Supplementary data associated with this article can be found in the online version at doi:10.1016/j.phrs.2024.107165.

References

[1] L.A. Smith, V.R. Cornelius, C.J. Plummer, G. Levitt, M. Verrill, P. Canney, A. Jones, Cardiotoxicity of anthracycline agents for the treatment of cancer: systematic review and meta-analysis of randomised controlled trials, BMC Cancer 10 (2010) 337, https://doi.org/10.1186/1471-2407-10-337.

[2] J. Marinello, M. Delcuratolo, G. Capranico, Anthracyclines as Topoisomerase II Poisons: From Early Studies to New Perspectives, Int J. Mol. Sci. 19 (11) (2018), https://doi.org/10.3390/ijms19113480.

[3] J.W. Harper, S.J. Elledge, The DNA damage response: ten years after, Mol. Cell 28 (5) (2007) 739–745, https://doi.org/10.1016/j.molcel.2007.11.015.

[4] S.Y. van der Zanden, X. Qiao, J. Neefjes, New insights into the activities and toxicities of the old anticancer drug doxorubicin, FEBS J. 288 (21) (2021) 6095–6111, https://doi.org/10.1111/febs.15583.

[5] K.B. Wallace, V.A. Sardao, P.J. Oliveira, Mitochondrial Determinants of Doxorubicin-Induced Cardiomyopathy, Circ. Res 126 (7) (2020) 926–941, https://doi.org/10.1161/CIRCRESAHA.119.314681.

[6] B.G. Childs, D.J. Baker, J.L. Kirkland, J. Campisi, J.M. van Deursen, Senescence and apoptosis: dueling or complementary cell fates? EMBO Rep. 15 (11) (2014) 1139–1153, https://doi.org/10.15252/embr.201439245.

[7] N. Nozaki, T. Shishido, Y. Takeishi, I. Kubota, Modulation of doxorubicin-induced cardiac dysfunction in toll-like receptor-2-knockout mice, Circulation 110 (18) (2004) 2869–2874, https://doi.org/10.1161/01.CIR.0000146889.46519.27.

[8] C. Henninger, G. Fritz, Statins in anthracycline-induced cardiotoxicity: Rac and Rho, and the heartbreakers, Cell Death Dis. 8 (1) (2017) e2564, https://doi.org/10.1038/cddis.2016.418.

[9] C. Hu, X. Zhang, N. Zhang, W.Y. Wei, L.L. Li, Z.G. Ma, Q.Z. Tang, Osteocrin attenuates inflammation, oxidative stress, apoptosis, and cardiac dysfunction in doxorubicin-induced cardiotoxicity, Clin. Transl. Med 10 (3) (2020) e124, https://doi.org/10.1002/ctm2.124.

[10] X. Zhang, C. Hu, C.Y. Kong, P. Song, H.M. Wu, S.C. Xu, Y.P. Yuan, W. Deng, Z. G. Ma, Q.Z. Tang, FNDC5 alleviates oxidative stress and cardiomyocyte apoptosis in doxorubicin-induced cardiotoxicity via activating AKT, Cell Death Differ. 27 (2) (2020) 540–555, https://doi.org/10.1038/s41418-019-0372-z.

[11] C. Hu, X. Zhang, P. Song, Y.P. Yuan, C.Y. Kong, H.M. Wu, S.C. Xu, Z.G. Ma, Q. Z. Tang, Meteorin-like protein attenuates doxorubicin-induced cardiotoxicity via activating cAMP/PKA/SIRT1 pathway, Redox Biol. 37 (2020) 101747, https://doi.org/10.1016/j.redox.2020.101747.

[12] F. Bernuzzi, S. Recalcati, A. Alberghini, G. Cairo, Reactive oxygen species-independent apoptosis in doxorubicin-treated H9c2 cardiomyocytes: role for heme oxygenase-1 down-modulation, Chem. Biol. Inter. 177 (1) (2009) 12–20, https://doi.org/10.1016/j.cbi.2008.09.012.

[13] T. Rharass, A. Gbankoto, C. Canal, G. Kursunluoglu, A. Bijoux, D. Panakova, A. C. Ribou, Oxidative stress does not play a primary role in the toxicity induced with clinical doses of doxorubicin in myocardial H9c2 cells, Mol. Cell Biochem 413 (1-2) (2016) 199–215, https://doi.org/10.1007/s11010-016-2653-x.

[14] B.B. Hasinoff, D. Patel, X. Wu, The oral iron chelator ICL670A (deferasirox) does not protect myocytes against doxorubicin, Free Radic. Biol. Med 35 (11) (2003) 1469–1479, https://doi.org/10.1016/j.freeradbiomed.2003.08.005.

[15] Y.L. Lyu, J.E. Kerrigan, C.P. Lin, A.M. Azarova, Y.C. Tsai, Y. Ban, L.F. Liu, Topoisomerase IIbeta mediated DNA double-strand breaks: implications in doxorubicin cardiotoxicity and prevention by dexrazoxane, Cancer Res 67 (18) (2007) 8839–8846, https://doi.org/10.1158/0008-5472.CAN-07-1649.

[16] E. Jirkovsky, A. Jirkovska, H. Bavlovic-Piskackova, V. Skalicka, Z. Pokorna, G. Karabanovich, P. Kollarova-Brazdova, J. Kubes, O. Lencova-Popelova, Y. Mazurova, M. Adamcova, A.R. Lyon, J. Roh, T. Simunek, P. Sterbova-Kovarikova, M. Sterba, Clinically Translatable Prevention of Anthracycline Cardiotoxicity by Dexrazoxane Is Mediated by Topoisomerase II Beta and Not Metal Chelation, Circ. Heart Fail 14 (11) (2021) e008209, https://doi.org/10.1161/CIRCHEARTFAILURE.120.008209.

[17] C.K. Tebbi, W.B. London, D. Friedman, D. Villaluna, P.A. De Alarcon, L.S. Constine, N.P. Mendenhall, R. Sposto, A. Chauvenet, C.L. Schwartz, Dexrazoxane-associated risk for acute myeloid leukemia/myelodysplastic syndrome and other secondary malignancies in pediatric Hodgkin's disease, J Clin Oncol 25(5) (2007) 493-500, doi:25/5/493 [pii]10.1200/JCO.2005.02.3879.

[18] M. Marty, M. Espie, A. Llombart, A. Monnier, B.L. Rapoport, V. Stahalova, Multicenter randomized phase III study of the cardioprotective effect of dexrazoxane (Cardioxane) in advanced/metastatic breast cancer patients treated with anthracycline-based chemotherapy, Ann. Oncol. 17 (4) (2006) 614–622.

[19] J. Huelsenbeck, C. Henninger, A. Schad, K.J. Lackner, B. Kaina, G. Fritz, Inhibition of Rac1 signaling by lovastatin protects against anthracycline-induced cardiac toxicity, Cell Death Dis. 2 (2011) e190, https://doi.org/10.1038/cddis.2011.65.

[20] M. Yoshida, I. Shiojima, H. Ikeda, I. Komuro, Chronic doxorubicin cardiotoxicity is mediated by oxidative DNA damage-ATM-p53-apoptosis pathway and attenuated by pitavastatin through the inhibition of Rac1 activity, J. Mol. Cell Cardiol. 47 (5) (2009) 698–705.

[21] Z. Acar, A. Kale, M. Turgut, S. Demircan, K. Durna, S. Demir, M. Meric, M.T. Agac, Efficiency of atorvastatin in the protection of anthracycline-induced cardiomyopathy, J. Am. Coll. Cardiol. 58 (9) (2011) 988–989, https://doi.org/10.1016/j.jacc.2011.05.025.

[22] A. Oesterle, U. Laufs, J.K. Liao, Pleiotropic Effects of Statins on the Cardiovascular System, Circ. Res 120 (1) (2017) 229–243, https://doi.org/10.1161/CIRCRESAHA.116.308537.

[23] J. Ma, Y. Wang, D. Zheng, M. Wei, H. Xu, T. Peng, Rac1 signalling mediates doxorubicin-induced cardiotoxicity through both reactive oxygen species-dependent and -independent pathways, Cardiovasc Res 97(1) (2013) 77-87, doi: cvs309 [pii]robo10.1093/cvr/cvs309.

[24] P.L. Hordijk, Regulation of NADPH oxidases: the role of Rac proteins, Circ. Res 98 (4) (2006) 453–462, https://doi.org/10.1161/01.RES.0000204727.46710.5e.

[25] O.A. Coso, M. Chiariello, J.C. Yu, H. Teramoto, P. Crespo, N. Xu, T. Miki, J. S. Gutkind, The small GTP-binding proteins Rac1 and Cdc42 regulate the activity of the JNK/SAPK signaling pathway, Cell 81 (7) (1995) 1137–1146, https://doi.org/10.1016/s0092-8674(05)80018-2.

[26] R. Perona, S. Montaner, L. Saniger, I. Sanchez-Perez, R. Bravo, J.C. Lacal, Activation of the nuclear factor-kappaB by Rho, CDC42, and Rac-1 proteins, Genes Dev. 11 (4) (1997) 463–475, https://doi.org/10.1101/gad.11.4.463.

[27] A.R. Simon, H.G. Vikis, S. Stewart, B.L. Fanburg, B.H. Cochran, K.L. Guan, Regulation of STAT3 by direct binding to the Rac1 GTPase, Science 290 (5489) (2000) 144–147, https://doi.org/10.1126/science.290.5489.144.

[28] C. Henninger, J. Huelsenbeck, S. Huelsenbeck, S. Grosch, A. Schad, K.J. Lackner, B. Kaina, G. Fritz, The lipid lowering drug lovastatin protects against doxorubicin-induced hepatotoxicity, Toxicol. Appl. Pharm. 261 (1) (2012) 66–73.

[29] C. Henninger, S. Huelsenbeck, P. Wenzel, M. Brand, J. Huelsenbeck, A. Schad, G. Fritz, Chronic heart damage following doxorubicin treatment is alleviated by lovastatin, Pharm. Res 91 (2015) 47–56, https://doi.org/10.1016/j.phrs.2014.11.003.

[30] J. Huelsenbeck, C. Henninger, A. Schad, K.J. Lackner, B. Kaina, G. Fritz, Inhibition of Rac1 signaling by lovastatin protects against anthracycline-induced cardiac toxicity, Cell Death Dis. 2 (8) (2011) e190, https://doi.org/10.1038/cddis.2011.65.

[31] Y. Gao, J.B. Dickerson, F. Guo, J. Zheng, Y. Zheng, Rational design and characterization of a Rac GTPase-specific small molecule inhibitor, Proc. Natl. Acad. Sci. USA 101 (20) (2004) 7618–7623.

[32] A. Shutes, C. Onesto, V. Picard, B. Leblond, F. Schweighoffer, C.J. Der, Specificity and mechanism of action of EHT 1864, a novel small molecule inhibitor of Rac family small GTPases, J. Biol. Chem. 282 (49) (2007) 35666–35678.

[33] S.C. Huelsenbeck, A. Schorr, W.P. Roos, J. Huelsenbeck, C. Henninger, B. Kaina, G. Fritz, Rac1 protein signaling is required for DNA damage response stimulated by topoisomerase II poisons, J. Biol. Chem. 287 (46) (2012) 38590–38599, https://doi.org/10.1074/jbc.M112.377903.

[34] J. Ohlig, C. Henninger, S. Zander, M. Merx, M. Kelm, G. Fritz, Rac1-mediated cardiac damage causes diastolic dysfunction in a mouse model of subacute doxorubicin-induced cardiotoxicity, Arch. Toxicol. 92 (1) (2018) 441–453, https://doi.org/10.1007/s00204-017-2017-7.

[35] F. Wartlick, A. Bopp, C. Henninger, G. Fritz, DNA damage response (DDR) induced by topoisomerase II poisons requires nuclear function of the small GTPase Rac, Biochim Biophys. Acta 1833 (12) (2013) 3093–3103, https://doi.org/10.1016/j.bbamcr.2013.08.016.

[36] C. Henninger, S. Pohlmann, V. Ziegler, J. Ohlig, J. Schmitt, G. Fritz, Distinct contribution of Rac1 expression in cardiomyocytes to anthracycline-induced cardiac injury, Biochem Pharm. 164 (2019) 82–93, https://doi.org/10.1016/j.bcp.2019.03.038.

[37] E. Christidi, L.R. Brunham, Regulated cell death pathways in doxorubicin-induced cardiotoxicity, Cell Death Dis. 12 (4) (2021) 339, https://doi.org/10.1038/s41419-021-03614-x.

[38] W.C. Claycomb, N.A. Lanson, Jr., B.S. Stallworth, D.B. Egeland, J.B. Delcarpio, A. Bahinski, N.J. Izzo, Jr, HL-1 cells: a cardiac muscle cell line that contracts and retains phenotypic characteristics of the adult cardiomyocyte, Proc Natl Acad Sci U S A 95(6) (1998) 2979-2984, doi:10.1073/pnas.95.6.2979.

[39] C. Garlanda, C. Parravicini, M. Sironi, M. De Rossi, R. Wainstok de Calmanovici, F. Carozzi, F. Bussolino, F. Colotta, A. Mantovani, A. Vecchi, Progressive growth in immunodeficient mice and host cell recruitment by mouse endothelial cells transformed by polyoma middle-sized T antigen: implications for the pathogenesis of opportunistic vascular tumors, Proc. Natl. Acad. Sci. USA 91 (15) (1994) 7291–7295, https://doi.org/10.1073/pnas.91.15.7291.

[40] Z. Kabaeva, M. Zhao, D.E. Michele, Blebbistatin extends culture life of adult mouse cardiac myocytes and allows efficient and stable transgene expression, Am. J. Physiol. Heart Circ. Physiol. 294 (4) (2008) H1667–H1674, https://doi.org/10.1152/ajpheart.01144.2007.

[41] P.L. Olive, Detection of DNA damage in individual cells by analysis of histone H2AX phosphorylation, Methods Cell Biol. 75 (2004) 355–373, https://doi.org/10.1016/s0091-679x(04)75014-1.

[42] R. Kitzinger, G. Fritz, C. Henninger, Nuclear RAC1 is a modulator of the doxorubicin-induced DNA damage response, Biochim Biophys. Acta Mol. Cell Res 1869 (10) (2022) 119320, https://doi.org/10.1016/j.bbamcr.2022.119320.

[43] D.A. Gewirtz, A critical evaluation of the mechanisms of action proposed for the antitumor effects of the anthracycline antibiotics adriamycin and daunorubicin, Biochem Pharm. 57 (7) (1999) 727–741, https://doi.org/10.1016/s0006-2952(98)00307-4.

[44] D. Cappetta, F. Rossi, E. Piegari, F. Quaini, L. Berrino, K. Urbanek, A. De Angelis, Doxorubicin targets multiple players: A new view of an old problem, Pharm. Res 127 (2018) 4–14, https://doi.org/10.1016/j.phrs.2017.03.016.

[45] O. Bergmann, S. Zdunek, A. Felker, M. Salehpour, K. Alkass, S. Bernard, S. L. Sjostrom, M. Szewczykowska, T. Jackowska, C. Dos Remedios, T. Malm,

M. Andra, R. Jashari, J.R. Nyengaard, G. Possnert, S. Jovinge, H. Druid, J. Frisen, Dynamics of Cell Generation and Turnover in the Human Heart, Cell 161 (7) (2015) 1566–1575, https://doi.org/10.1016/j.cell.2015.05.026.
[46] M. Rasanen, J. Degerman, T.A. Nissinen, I. Miinalainen, R. Kerkela, A. Siltanen, J. T. Backman, E. Mervaala, J.J. Hulmi, R. Kivela, K. Alitalo, VEGF-B gene therapy inhibits doxorubicin-induced cardiotoxicity by endothelial protection, Proc. Natl. Acad. Sci. USA 113 (46) (2016) 13144–13149, https://doi.org/10.1073/pnas.1616168113.
[47] K. Rothkamm, M. Lobrich, Evidence for a lack of DNA double-strand break repair in human cells exposed to very low x-ray doses, Proc. Natl. Acad. Sci. USA 100 (9) (2003) 5057–5062, https://doi.org/10.1073/pnas.0830918100.
[48] S.P. Jackson, J. Bartek, The DNA-damage response in human biology and disease, Nature 461 (7267) (2009) 1071–1078, https://doi.org/10.1038/nature08467.
[49] S. Sengupta, C.C. Harris, p53: traffic cop at the crossroads of DNA repair and recombination, Nat. Rev. Mol. Cell Biol. 6 (1) (2005) 44–55, https://doi.org/10.1038/nrm1546.
[50] D. Sanchis, M. Mayorga, M. Ballester, J.X. Comella, Lack of Apaf-1 expression confers resistance to cytochrome c-driven apoptosis in cardiomyocytes, Cell Death Differ. 10 (9) (2003) 977–986, https://doi.org/10.1038/sj.cdd.4401267.
[51] Y. Maejima, S. Adachi, H. Ito, K. Hirao, M. Isobe, Induction of premature senescence in cardiomyocytes by doxorubicin as a novel mechanism of myocardial damage, Aging Cell 7 (2) (2008) 125–136, https://doi.org/10.1111/j.1474-9726.2007.00358.x.
[52] P. Lassus, P. Roux, O. Zugasti, A. Philips, P. Fort, U. Hibner, Extinction of rac1 and Cdc42Hs signalling defines a novel p53-dependent apoptotic pathway, Oncogene 19 (20) (2000) 2377–2385, https://doi.org/10.1038/sj.onc.1203553.
[53] R. Wang, Q. Yu, X. Wang, B. Li, A. Ciotkowska, B. Rutz, Y. Wang, C.G. Stief, M. Hennenberg, Rac1 silencing, NSC23766 and EHT1864 reduce growth and actin organization of bladder smooth muscle cells, Life Sci. 261 (2020) 118468, https://doi.org/10.1016/j.lfs.2020.118468.
[54] J.Y. Byun, C.H. Yoon, S. An, I.C. Park, C.M. Kang, M.J. Kim, S.J. Lee, The Rac1/MKK7/JNK pathway signals upregulation of Atg5 and subsequent autophagic cell death in response to oncogenic Ras, Carcinogenesis 30 (11) (2009) 1880–1888, https://doi.org/10.1093/carcin/bgp235.
[55] S.C. Huang, Y.M. Chen, Y.Y. Hu, Y.J. Shi, Q.W. Xiao, Z. Li, J.L. Kang, Q. Zhou, G. Shen, H.Y. Jia, Downregulation of MCF2L Promoted the Ferroptosis of Hepatocellular Carcinoma Cells through PI3K/mTOR Pathway in a RhoA/Rac1 Dependent Manner, Dis. Markers 2022 (2022) 6138941, https://doi.org/10.1155/2022/6138941.
[56] A. Rufini, P. Tucci, I. Celardo, G. Melino, Senescence and aging: the critical roles of p53, Oncogene 32 (43) (2013) 5129–5143, https://doi.org/10.1038/onc.2012.640.
[57] M.S. Siddiqui, M. Francois, M.F. Fenech, W.R. Leifert, Persistent gammaH2AX: A promising molecular marker of DNA damage and aging, Mutat. Res Rev. Mutat. Res 766 (2015) 1–19, https://doi.org/10.1016/j.mrrev.2015.07.001.
[58] F. Rodier, J.P. Coppe, C.K. Patil, W.A. Hoeijmakers, D.P. Munoz, S.R. Raza, A. Freund, E. Campeau, A.R. Davalos, J. Campisi, Persistent DNA damage signalling triggers senescence-associated inflammatory cytokine secretion, Nat. Cell Biol. 11 (8) (2009) 973–979, https://doi.org/10.1038/ncb1909.
[59] L.K. Booth, R.E. Redgrave, O. Folaranmi, J.H. Gill, G.D. Richardson, Anthracycline-induced cardiotoxicity and senescence, Front Aging 3 (2022) 1058435, https://doi.org/10.3389/fragi.2022.1058435.
[60] M.A. Mitry, D. Laurent, B.L. Keith, E. Sira, C.A. Eisenberg, L.M. Eisenberg, S. Joshi, S. Gupte, J.G. Edwards, Accelerated cardiomyocyte senescence contributes to late-onset doxorubicin-induced cardiotoxicity, Am. J. Physiol. Cell Physiol. 318 (2) (2020) C380–C391, https://doi.org/10.1152/ajpcell.00073.2019.

Further reading

[61] B.L. Montalvo-Ortiz, L. Castillo-Pichardo, E. Hernandez, T. Humphries-Bickley, A. De la Mota-Peynado, L.A. Cubano, C.P. Vlaar, S. Dharmawardhane, Characterization of EHop-016, novel small molecule inhibitor of Rac GTPase, J. Biol. Chem. 287 (16) (2012) 13228–13238, https://doi.org/10.1074/jbc.M111.334524.
[62] L. Hong, S.R. Kenney, G.K. Phillips, D. Simpson, C.E. Schroeder, J. Noth, E. Romero, S. Swanson, A. Waller, J.J. Strouse, M. Carter, A. Chigaev, O. Ursu, T. Oprea, B. Hjelle, J.E. Golden, J. Aube, L.G. Hudson, T. Buranda, L.A. Sklar, A. Wandinger-Ness, Characterization of a Cdc42 protein inhibitor and its use as a molecular probe, J. Biol. Chem. 288 (12) (2013) 8531–8543, https://doi.org/10.1074/jbc.M112.435941.
[63] K. Zins, T. Lucas, P. Reichl, D. Abraham, S. Aharinejad, A Rac1/Cdc42 GTPase-specific small molecule inhibitor suppresses growth of primary human prostate cancer xenografts and prolongs survival in mice, PLoS One 8 (9) (2013) e74924, https://doi.org/10.1371/journal.pone.0074924.
[64] X. Shang, F. Marchioni, N. Sipes, C.R. Evelyn, M. Jerabek-Willemsen, S. Duhr, W. Seibel, M. Wortman, Y. Zheng, Rational design of small molecule inhibitors targeting RhoA subfamily Rho GTPases, Chem. Biol. 19 (6) (2012) 699–710, https://doi.org/10.1016/j.chembiol.2012.05.009.
[65] T. Ishizaki, M. Uehata, I. Tamechika, J. Keel, K. Nonomura, M. Maekawa, S. Narumiya, Pharmacological properties of Y-27632, a specific inhibitor of rho-associated kinases, Mol. Pharm. 57 (5) (2000) 976–983.